Strength of Flocs Formed by the Complexation of Proteins and Humic Acid

January 2021

WAN KHAIRUNNISA BINTI WAN ABDUL KHODIR

Strength of Flocs Formed by the Complexation of Proteins and Humic Acid

A dissertation submitted to

the Graduate School of Life and Environmental Sciences,

the University of Tsukuba

in partial Fulfilment of the Requirements

for the Degree of Doctor of Philosophy in Bioresource Engineering

(Doctoral Program in Appropriate Technology and Sciences for Sustainable Development)

WAN KHAIRUNNISA BINTI WAN ABDUL KHODIR

Table of Contents

List of Figure

List of Table

1 General Introduction and Research Goal

1.1 Colloidal particles in the environment

Colloidal substances are roughly from nanometer to micrometer in size and exist in dynamic systems (Lead and Wilkinson, 2007). In soil and water environments, most of the colloidal substances are clays and organic materials (Bünemann et al. 2018). These natural colloidal materials usually bear electrical charges on their surfaces. The amount of positive and/or negative charges depends on the environmental conditions such as pH of the medium, ionic strength, and concentration of the substances. The soil colloidal substances (e.g., humic substances, protein, and polysaccharides) have a property of binding to the different colloidal substances such as synthetic particles through several physical and chemical processes. These processes are referred to adsorption, coagulation, aggregation, and dispersion which could amplify the chemical activity, transportation action, and hydraulic properties of the substances (Giachin et al. 2017).

Electrostatic interaction, van der Waals forces, hydration phenomenon, and hydrodynamic interaction are the interactions involved in maintaining the stability of colloid. In meanwhile, an attractive force between colloidal substances can form aggregation. Considering the van der Waals force and diffuse double - layer interaction in determining the stability of colloids is referred to as classical DLVO (Derjaguin, Landau, Verwey, Overbeek) theory (Verwey 1947; Trefalt and Borkovec 2014a).

One of the characteristics of colloids in the natural environmental condition is charging behavior of the substances. This is an important aspect of controlling the aggregation and dispersion of colloidal suspensions. For example is the adsorption induced by charged ions, polyelectrolytes, clay and, surfactant (Kobayashi 2008; Beltrán-Heredia and Sánchez-Martín 2009). Reaching the point of zero charges, known as an isoelectric point (IEP), points out the start of the aggregation process. Charge reversal also known as overcharging usually occurs

because of saturated adsorption of oppositely charged substances. There are additional attractive interactions, such as hydrophobic or van der Waals force, that occurs between the substances. Therefore, the interaction between colloidal substrate in the soil and water environment must be paid attention to consider especially when these interactions could affect the mobility of substances.

1.2 Transportation of colloidal matter in soil and water environment

Colloidal substances with pollutants in the environment have the potential to move with the water flow. In the worst-case scenario, the unsupervised situation can enhance the transport of pollutants, which leads to further contamination. The movement of such colloidal substances through soil pore entirely depends on the size of the substances (Hajra et al. 2002; Li et al. 2018; Oladoja and Pan 2015; Kobayashi 2005). For colloids to be mobile in soil pore, they must be stable, and the pore is larger than the colloid substances. Meanwhile, larger substances easily settle and deposit to the soil matrix. Other than the size of substances, the size of soil pore is also the factor in the mobilization of colloid (Enfield and Bengtssona 1988). The interaction between the substances also plays an important role in the aggregation of substances. The collision between primary substances and their interaction depends on the flow field (Kobayashi 2005; Hakim and Kobayashi 2019). The high shear flow would cause the breakage of the aggregated complex and permits the mobilization of substances in the soil environment. In a meanwhile, if the shear flow is low, the aggregated substances would not break and are retained in the pore.

1.3 Floc breakage and floc strength

The strength of flocs depends on the inter-substance binding forces in the aggregates to hold the flocs together (Parker 1972; Bache et al. 1997). The floc strength is also referring to the number of individual bonds and their strength within the flocs. The floc strength study was conducted through a converging flow field. The floc strength method can provide an insight into the strength of the binding forces between the flocs and controlling its parameter in the environment

1.4 Humic substances

Humic substances (HSs) are the significant fraction of natural organic matter (NOM) in soil and water environments comprised of degraded matters of bacterial matter, plant, and animal products. The HSs play an essential aspect in the nutrient sequence system and the transportation of pollutant or hydrophobic organic contaminants, metal ion, and radionuclides in the soil and water environment (Giachin et al. 2014, 2017).

The HSs are easily bound with the mineral surfaces (Ma et al. 2018), ions (Brigante et al. 2009; Hakim et al. 2019), organic molecules (Tan et al. 2008; Khodir et al. 2020; Santos et al. 2011), oxides (Pota et al. 2020), and polymer (Xu et al. 2011). HSs such as humic acid (HA) and fulvic acid (FA) are high molecular mass polymer. These HSs are considered a supramolecular organization composed of functional groups (carboxylic acid, phenolic acid), aliphatic carbon, polymethylenes (-CH2-), O, N, S, and P atoms, and others. The HSs composition has led to various interactions such as electrostatic interaction, hydrophobic interaction, van der Waals interaction, and hydrogen bonding (Brigante et al. 2009; Avena and Wilkinson, 2002). The composition of carboxyl, phenolic, and carbon content of LHA obtained from International Humic Substances Society (IHSS) is displayed in Table 1.1 below.

Table 1.1. Selected composition of LHA sample used in this thesis as reported by IHSS

IHSS sample	Carboxyl (meq $g^{-1}C$)	Phenolic (meq $g^{-1}C$)	Carbon content % (w/w)	Aromatic carbon (peak area percentages) (165-110 ppm)
Leonardite humic acid (1S104H)	7.46	2.31	63.81	58

1.5 Lysozyme protein

To explore the relationship between HSs and protein, a detailed and well-organized framework is needed. It is essential to use a characterized and readily available such as Lysozyme (LSZ) protein. LSZ is a globular protein with an ellipsoidal shape with a molecular weight of 14.3 kDa and an isoelectric point near pH 11. Moreover, LSZ protein is positively charged substances with the size (radius) around 1.64 nm (Dabkowska et al. 2018). The LSZ is well known for the high structural stability that makes it useful as a model protein for many practical uses and widely studied. Unfortunately, the knowledge of the interaction between the natural particles is lacking. LSZ protein is a weak polyelectrolyte, so do the HSs.

1.6 Moringa oleifera seed protein

Moringa oleifera (MO) is a plant mainly found around the tropical country and currently commercializes in several industries such as food, pharmaceutical, and cosmetic. Due to its potential properties, MO seed (Figure 1.4) gains attention from researchers for its coagulating abilities. Unfortunately, a problem of using natural coagulant is the method of extraction and purification. There are several extraction and purification methods used previously. Due to protein solubility, the MO seed powder can use the water or salt solution to extract the protein. Some of the purification methods used are dialysis, free-drying, ion-exchange, delipidation, precipitation, and centrifugation (Yamaguchi et al. 2020). Details on

the extraction and purification method and the molecular weight obtained are displayed in Table 1.2.

Table 1.2. The extraction and purification methods from MO seed reported by previous researchers (Yamaguchi et al. 2020)

Extraction method	References	Molecular weight (kDa)
Water extract	Ndabigengesere et al. 1995; Santos et al. 2005	13, 20
Fractionated extract (salt)	Santos et al. 2009	26.5
Purified extract (phosphate)	Agrawal et al. 2007	66
Deoiled purified extract (water and salt)	Ghebremichael et al. 2005	Less than 6.5 for both extract
Purified defatted extract (phosphate)	Gassenschmidt et al. 1995	6.5
Purified extract (saline)	Okuda et al. 2001	3
Purified lectin protein: from seed and NCBI database	Katre et al. 2008; Abd Wahid et al. 2017	14, 8

*NCBI = National Center for Biotechnology Information

Therefore, in this study, we focused on the strength of flocs formed by protein and HS. The floc strength depends on the intermolecular binding within and between the aggregates. The interaction between substances influences the inter-and intra- molecular binding of floc. The physicochemical factors such as ionic strength, pH, and mass ratio can influence the interaction between substrates.

2 Characteristic of proteins and humic acid

2.1 Introduction

The charging behavior of colloidal particles, either positive or negative, depends on the solution chemistry. The surface charge of colloidal particles affects the interaction between particles, thus controls the aggregation-dispersion of colloidal suspensions. The aggregation of colloidal particles usually occurs at charge neutralization conditions and high salt concentration. Polyelectrolytes interact strongly with the oppositely charged colloidal particles to modify the surface properties and the interaction forces acting between colloidal particles. However, most colloidal particles do not carry a constant surface potential, which depends on the salt concentration and pH. For such particles, the surface potential and charge density should be known. We attempt to summarize the charging behavior of individual material such as protein (Lysozyme and *Moringa oleifera* seed) and humic acid (LHA) through literature on charge density and EPM. Since the ionization of weak particles partially occurs, it is crucial to identify individual surface charge density as a pH and ionic strength function.

The electrophoretic mobility (EPM) represents the magnitude of the surface potential of a particle. Several theories, such as Smoluchwoski (Smoluchowski 1903), and Huckel, have quantified the surface potential by converting the EPM values to zeta potential. However, these theories ignored the relaxation effect and suitable for low surface potential only (Kobayashi 2008). Therefore, we discussed the zeta potential of MO seed protein in the presence of salt based on Smoluchowski and Huckel theories.

Other than electrokinetic properties, the particle size of the colloidal particle can affect the aggregation process. Large particles quickly formed floc compared to the smaller particle. In the flocculation process, the adsorption depends on the particle size (Hogg 2012). Therefore, the particle size is an important parameter to consider. This chapter outlined some of the characteristics of LSZ protein, MO seed protein, and LHA.

2.2 Method

2.2.1 Preparation of Moringa oleifera powder

Moringa oleifera (MO) seed from Minh Tue Company (Hanoi, Vietnam) was used in this experiment. Deshelled seeds of MO were oven-dried at 40 °C for one week before being ground into powdered seeds. The powdered MO seed was infused with deionized water (Elix, Milipore) to prepare the MO seed protein stock solution. Prior to the filtration with a filter paper (DISMIC 25HP 0.2 μm, ADVANTEC), the MO seed suspension was thoroughly shaken for 15 minutes.

2.2.2 Bradford Assay

Bradford assay was used to analyze the protein concentration from the extracted MO seed. The protein standard curve was prepared by using Bovine Serum Albumin (BSA, BIO-RAD) standard. The solubilized protein concentration was then measured at 595 nm by using UV-Vis Spectrophotometer (UV-1650PC, Shimadzu). By using a similar procedure, the MO seed protein solution was measured.

2.2.3 Dynamic Light Scattering measurement

The MO protein size was determined by using the dynamic light scattering (DLS) measurement (Zetasizer Nano ZS apparatus, Malvern). For reliable size measurement data, the comparison between the two conditions was applied. The conditions were (i) direct DLS measurement from fresh MO stock solution (no second filtration) and (ii) second filtration before the DLS measurement. In condition (ii), the MO seed stock solution was filtered with 0.2 μm filter paper.

2.2.4 Electrophoretic mobility measurement

We measured the electrophoretic mobilities of 0.05 g/L (w/v) MO seed suspension in the presence of KCl at 20 ℃ with a Zetasizer Nano ZS apparatus (Malvern). The electrophoretic mobility was measured for MO solution at 0.5 mM, and 0.1 M KCl concentrations as a function of pH ranged from pH 3 to pH 10. For the adjustment of pH, HCl and KOH solution was used. The measurement was performed in triplicate for each sample and carried out at 20 ℃. Smoluchowski and Huckel equations were used in this mobility measurement.

2.2.5 Estimation of surface charge density

2.2.5.1 Surface charge density of LHA

The proton-binding curve of an HS is measured based on the carboxyl and phenolic groups. Considering the HS as a fusion of monoprotic acid, each titration point was assessed based on the electroneutrality equation below

$$\sum_i [Org_i^-] = [Na^+] + [H^+] - [Cl^-] - [OH^-] \quad (1)$$

where $[Na^+]$ and $[Cl^-]$ are dilution-corrected concentrations of added NaOH and HCl (used by Ritchie and Perdue (2003)), and $[Org_i^-]$ is the dilution-corrected concentration of the *i*th organic anion in the sample.

Table 2.1. The fitting parameters of modified Henderson-Hasselbalch for Leonardite humic acid

Sample	Q_1	Q_2	K_1	K_2	n_1	n_2
LHA	8.17	1.13	4.59	9.72	3.32	1.31

Where Q_1 and Q_2 are the concentration of the binding sites, K_1 and K_2 are the mean K values for proton binding, n_1 and n_2 are the empirical parameters that control the width of proton binding sites.

The charge density of LHA can be calculated from the modified Henderson-Hasselbalch equation (Katchalsky and Spitnik 1947) for carboxyl and phenolic-binding site using the parameters in Table 2.1.

$$Q_{TOT} = \left(\frac{Q_1}{1 + (K_1[H^+])^{1/n_2}}\right) + \left(\frac{Q_2}{1 + (K_2[H^+])^{1/n_2}}\right) \quad (2)$$

where Q_{TOT} represented in unit of meq gC^{-1} by fitting all the parameters from Table 2.1.

2.2.5.2 Surface charge density of LSZ

The estimation of surface charge density was taken from charge amount obtained from proton titration by Tan et al. (2008) and Kuehner et al. (1999). The surface charge density σ was obtained by dividing the sum of charge by surface area (3.8×10^{-17} m^2 for oval sphere). This method was followed from Yamaguchi and Kobayashi (2016).

2.2.5.3 Zeta potential analysis

The measured value of electrophoretic mobility μ can be converted to zeta potential ζ (particle surface potential) by using Smoluchowski equation

$$\mu = \frac{\varepsilon_r \varepsilon_0}{\eta} \zeta \quad (3)$$

where ε_r is a relative permittivity and ε_0 is a vacuum permittivity, meanwhile, η is a viscosity of the electrolyte solution. κ is the Debye-Huckel parameter defined by

$$\kappa = \left(\frac{2n^{\infty} z^2 e^2}{\varepsilon_r \varepsilon_0 kT}\right)^{1/2} \quad (4)$$

k is the Boltzman constant, *T* is the absolute temperature, *e* is the elementary electrical charge, and *n* is the concentration of *z:z* electrolyte. In this study, *z* = 1 for KCl.

The zeta potential is expressed by Hückel expression (Hückel, 1924);

$$\zeta = \frac{3\,\eta}{2\varepsilon_r \varepsilon_0}\mu \tag{5}$$

Both equations by Smoluchowski (eq. 3) and Hückel (eq. 5) were compared to see the presence of the electrical double layer (EDL) relaxation effect.

2.3 Result and Discussions

2.3.1 Charge density of LSZ and LHA

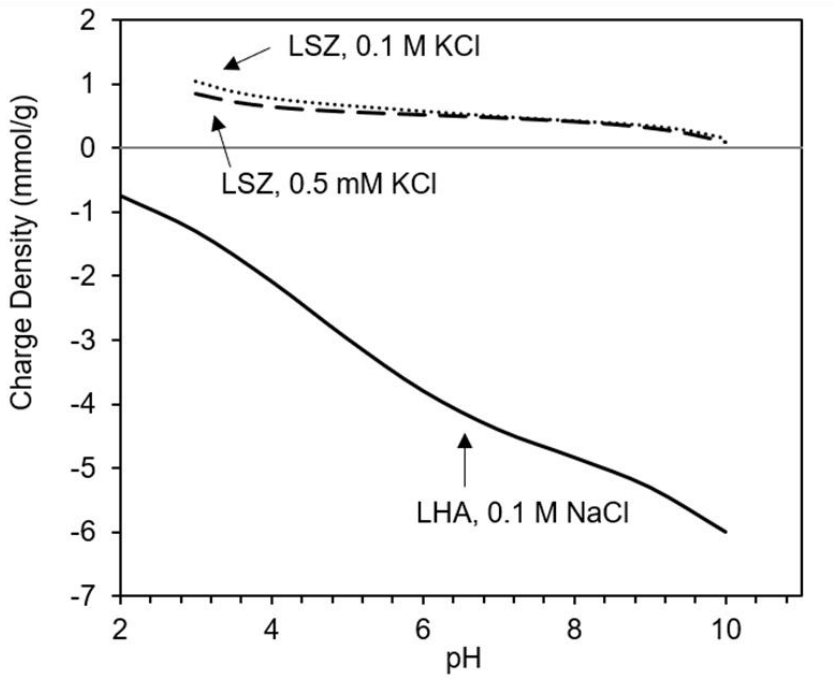

Figure 2.1. Surface charge density of LSZ (0.5 mM and 0.1 M KCl) and LHA (0.1 M NaCl) as a function of pH (Khodir et al. 2020)

The charge density of LSZ is influenced by ionic strength at a lower pH than at higher pH. Tan et al. (2008) reported reducing positive charge density of LSZ measured using Mutek

potential. This reduction in LSZ charge density occurs because of the dissociation and deprotonation effect because of the presence of amino acid residues. The LHA also encountered a similar effect of protonation and deprotonation. The presence of carboxylic and phenol groups caused the LHA to easily influence by pH.

2.3.2 Bradford Assay

The standard curve of a BSA protein at different protein concentrations is as shown in Figure A1. The measured absorbance of MO protein was compared with the standard curve of BSA protein. We obtained 0.026 and 1.13 mg/ml of protein for 0.05 g/L (w/v), and 2.4 g/L (w/v), consequently, as displayed in Table 2.2.

Table 2.2. MO seed protein concentration measured using the Bradford assay with absorbance at 595 nm.

MO seed protein concentration, g/L	Measured protein concentration, mg/mL
0.05	0.026
2.4	1.13

2.3.3 Dynamic Light Scattering measurement of MO protein

2.3.3.1 Effect of pH

The DLS measurement in Figure 2.2 obtained 24.17 nm at pH 3.2 for condition (i), while condition (ii) obtained 6.66 nm at the same pH value. The DLS measurement for the MO suspension in condition (i) is much more prominent in size than the MO suspension in condition (ii).

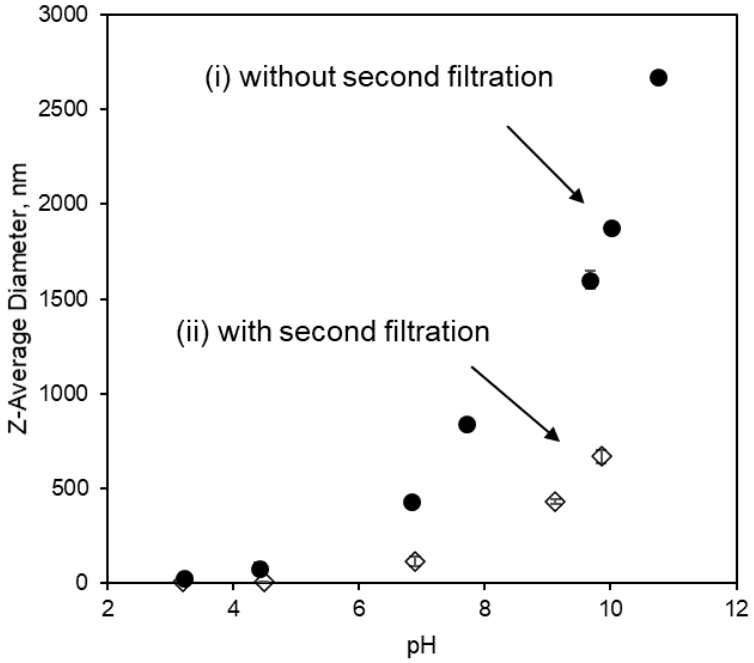

Figure 2.2. Z-average diameter of 2.4 g/L MO suspension of two conditions: (i) no second filtration (from fresh sample), and (ii) with second filtration before DLS measurement. The DLS measurement was plotted against pH from pH 3 to pH 11.

The observation on the MO suspension was performed macroscopically and microscopically as shown in Figure 2.3. The mixture suspension at pH 3.2 with a clear mixture at the beginning became cloudy over time. After 24 hours of observation, the sediments were formed for pH 7.7 and above. The formation of aggregation at higher pH suggested the MO seed suspension might contain protein, carbohydrate, lignin, and fatty acid (Ndabigengesere et al. 1995).

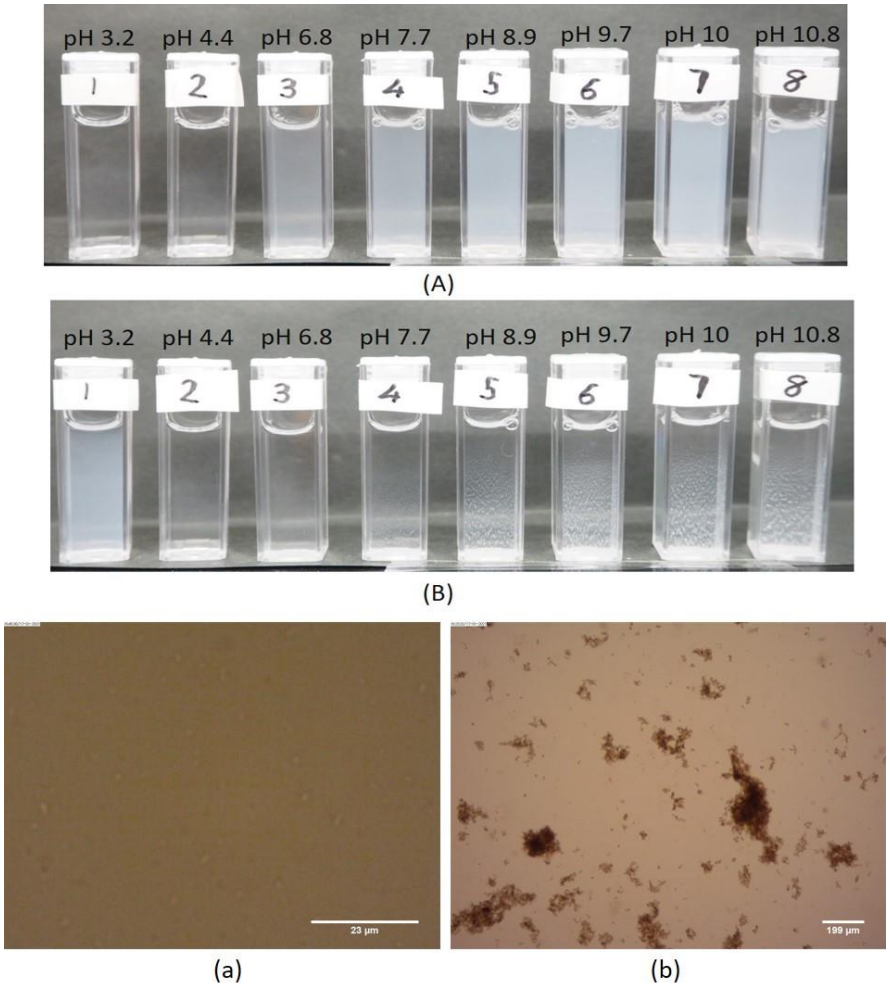

Figure 2.3. A 24-hours observation on the 2.4 g/L (w/v) MO suspension of condition (i) with no KCl at a function of pH. The pictures were taken with a time frame of 0 hour (A), and 24 hours (B). Total volume used was 3 mL Below is the microscopic observation after 24-hours for suspension of bottle 8 (a) and bottle 1 (b). Image of bottle 8 was captured at 4x magnification, meanwhile the image of bottle 1 was captured at 100x magnification.

2.3.3.2 Effect of KCl concentration

By using the MO suspension of condition (ii), the effect of KCl concentration was measured. Figure 2.4 and Table A2 (Appendix) showed the z-average diameter of bare MO as a function of KCl concentration, 0.5 mM, 1 mM, 10 mM, and 50 mM. In this experiment, we obtained 5.84 nm without the influence of salt. The average diameter of the MO protein was detected to increase with the addition of KCl concentration.

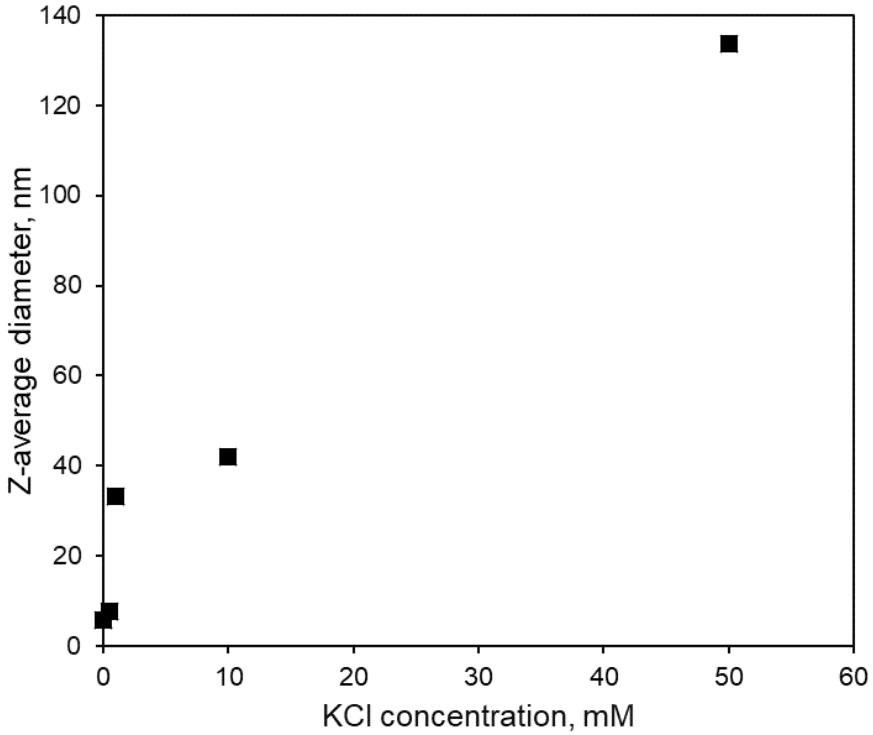

Figure 2.4. Z-average diameter of 2.4 g/L (w/v) MO suspension with the second filtration (condition ii) as a function of KCl concentration.

2.3.4 Charging behavior of proteins and humic acid

2.3.4.1 Zeta potential of MO seed suspension

Figure 2.5 demonstrates the zeta potential of the MO protein suspension on the effect of KCl concentrations of 1 mM and 30 mM. The MO suspension was measured using Smoluchowski and Huckel equation. Figure 2.5 and 2.6 shows the effect of double-layer relaxation. This effect appears at lower pH and is displayed in Figure 2.5. The relaxation effect occurs from the addition of salt, where the retardation of ion cloud is apparent.

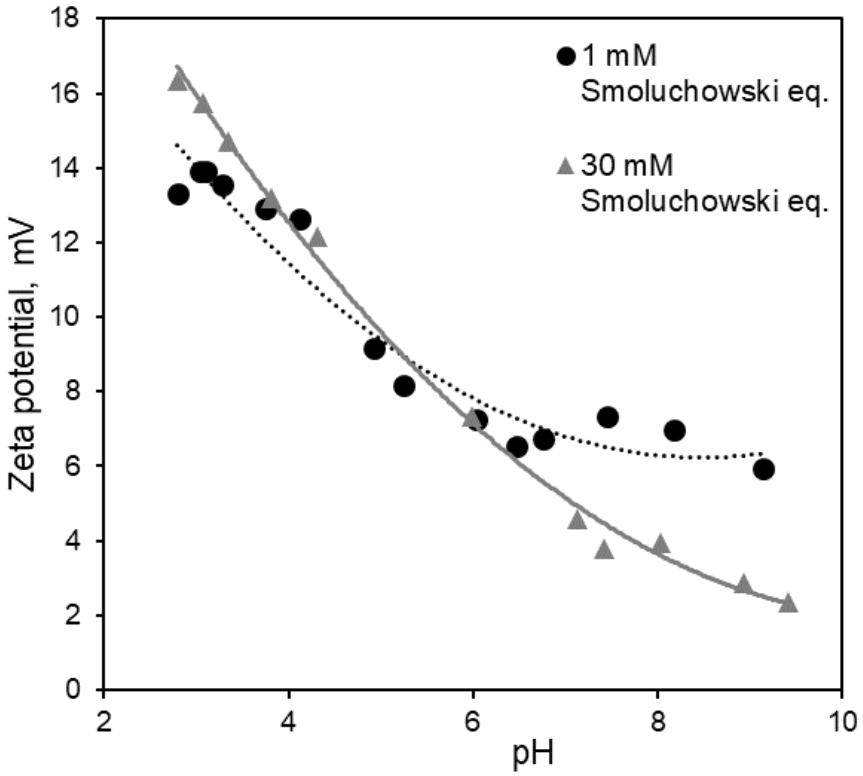

Figure 2.5. Zeta potential of MO seed protein at 1 mM and 30 mM KCl concentrations over a range of pH. The values calculated by the Smoluchowski equation.

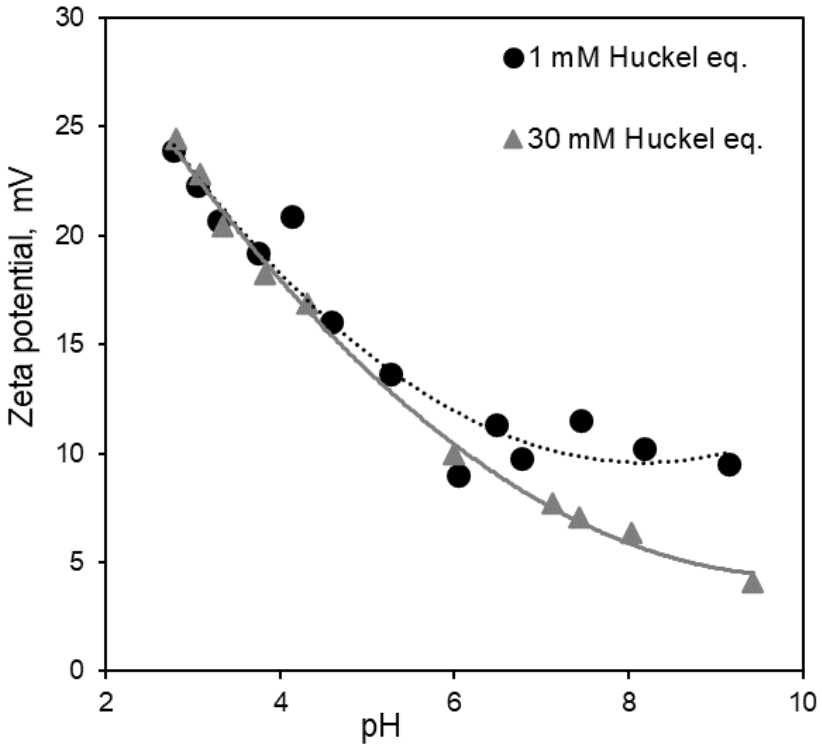

Figure 2.6. Zeta potential of MO seed protein at 1 mM and 30 mM KCl concentrations over the pH. The values calculated by the Huckel equation.

2.4 Conclusion

In this chapter, the characteristic of Lysozyme (LSZ), *Moringa oleifera* (MO) seed protein, and Leonardite humic acid (LHA) was analyzed. These substances were analyzed for particle size, zeta potential, and protein concentration using Bradford assay. Some of the data were extracted from the literature as well. Below is a summary of this chapter.

1) We obtained the 0.026 mg/L and 1.13 g/L for 0.05 g/L and 2.4 g/L of MO suspension, respectively. The protein concentration of MO suspension was measured using Bradford assay.
2) The size of MO suspension was measured based on two conditions; (i) direct measurement and (ii) application of secondary filtration. We obtained 24.17 nm and 6.66 nm at pH 3.2 for conditions (i) and (ii), consequently. Even though both conditions

show differences in hydrodynamic size, the data display increased aggregation at high pH. The macroscopic and microscopic observation supported this data.

3) The relaxation effect was detected for the Smoluchowski equation that did not consider this effect. The relaxation effect on MO suspension was only detected at low pH between 1 mM and 30 mM KCl.
4) The charging behavior of LSZ, LHA, and MO seed protein was measured using electrophoretic mobility (EPM). The pH and ionic strength easily influenced all the substances due to amino acid and carboxyl groups.

3 Strength of floc complex of LSZ protein and LHA

3.1 Introduction

In the movement of particles through the soil pore following the water flow, the hydrodynamic forces might promote aggregation or disaggregation of a floc. Aggregation and disaggregation of floc would influence transportation (Ouyang et al. 1996). Humic acid (HA) is readily adsorbed to different types of particles thus, it can regulate the transportation of colloid or colloid-associated contaminants. Other macromolecules in the environment are proteins. Protein consists of hydrophobic/ hydrophilic and positive and negative charges, generating a complex interaction with other particles (Giachin et al. 2014; Rigou et al. 2006). A protein is also considered part of natural organic matter (NOM) in the soil. The complexity of the various types of interactions causes extreme difficulty in predicting the interaction of a given protein with a different component of soil surfaces (Rigou et al. 2006). Hence, the interaction between protein and humic acid is the focus of this thesis. Several previous research has studied the interaction between protein and HA.

Lysozyme (LSZ) was chosen as the model protein because of the stability properties. The interaction study on the LSZ and HA by Tan has concluded the charge neutralization is the primary mechanism. They also obtained the largest size of aggregates produced at low salt concentration. Despite the impressive outcome, more analysis is needed. DLS technique used in their research has limitations in particle size determination (Li et al. 2018). Further research on this complex leads to transportation study. Li et al. (2013; 2018) pinpointed the importance of characteristics of floc in transportation. However, a more systematic study is needed to analyze the properties of protein – humic acid complex.

Floc strength is an important parameter to study the transportation of particles in soil pore. A study on the floc strength has recently been reported by (Hakim and Kobayashi 2019; Hakim

et al. 2019; Khodir et al.2020). They focused on the effect of a divalent cation, pH, tail length of surfactant, and hydrophobicity on the humic acid aggregates. They found the hydrophobicity enhances the formation of aggregates and how the forces influence the humic acid behavior. However, they did not investigate the effect of ionic strength, mass ratio, and the floc strength of protein – humic acid complex. Taking these parameters into account, the floc strength of protein – humic acid complex is the main focus of this thesis. Also, we covered the effect of mass ratio, pH, and ionic strength on LSZ and HA complexes.

3.2 Experimental

3.2.1 Material

Leonardite humic acid of the International Humic Material Society (IHSS) (LHA, IS104H, Bowman County, ND, USA) was used. At 65 °C overnight, the LHA powder was oven-dried to eliminate moisture. The dried LHA powder was dissolved with a KOH solution to prepare the LHA stock solution (0.25 wt%) (Wako Pure Chemical Industries). According to IHSS, COOH groups contain 4.76 mmol/g of LHA. An equivalent amount or more of KOH of a humic acid carboxylic group was needed to fully dissolve the LHA powder (Hakim and Kobayashi 2018). The deionized water (Elix, Milipore) was used to dilute the prepared stock solution and the stock was kept at 4 ◦C.

Lysozyme (LSZ) protein (Sigma Aldrich, L6876-10G) was used in the experiment. The lysozyme solution was used directly without further purification. The stock solution of LSZ was prepared every two weeks to maintain its freshness and stored at 4 °C.

An inorganic salt KCl (Wako Pure Chemical Industries) was used in this experiment to study the influence of ionic strength on the formation of floc and strength. Moreover, HCl and KOH solutions (Wako Pure Chemical Industries) were prepared as the pH adjuster. All the

solutions prepared were degassed with a vacuum pump (GCD-051X, ULVAC) to avoid CO_2 contamination during the analysis.

3.2.2 Method

3.2.2.1 Electrophoretic measurement

The electrophoretic mobility (EPM) of LSZ–LHA complexes in different KCl concentrations (3 mM, 10 mM, and 50 mM) as a pH function was measured. The LHA was sonicated previously for 15 min in the cold condition to prevent aggregation amongst LHAs interaction with LSZ. All the suspension used in the experiment has been degassed before use. The EPM was measured for 24-hours suspension. The mass ratio of the LSZ–LHA suspension was described as C_{LSZ}/C_{LHA}, where C represents the mass concentration of the substance. The concentration of LHA was set to 10 mg/L during the experiment, and the concentration of LSZ was accustomed to obtain mass ratio C_{LSZ}/C_{LHA} = 2.5 and 5. Meanwhile, the concentrations of LSZ at mass ratio 2.5 and 5 were 25 mg/L and 50 mg/L, respectively.

3.2.2.2 Microscopic and macroscopic observation on the lysozyme protein-humic acid aggregates

The visual observation was performed for the aggregation-dispersion of LSZ-LHA complex at different KCl concentrations. The inspection was performed macroscopically and microscopically as a function of pH. The pH was adjusted with HCl or KOH to reach the required pH around pH 3 – 8. The ratio of C_{LSZ}/C_{LHA} solution was adjusted for mass ratio 2.5, where LHA concentration was fixed at 10 mg/L for every measurement. A series of bottles (e.g., 3 mM at pH 3 – 8) were photographed by using a camera (Olympus PEN Lite, E-PL 7) for every 30 minutes. This is for macroscopic observation to check the aggregation-sedimentation state at various KCl concentration and pH. Meanwhile, the microscopic observation was performed through a microscope (Shimadzu BA210E, Moticam 580INT).

3.2.2.3 Strength of the LSZ-LHA complex

The illustration of floc breakage through a converging flow field experiment was shown in Figure 3.1. The mixture of LSZ-LHA suspension was prepared as in the above description. After 24 hours of settled aggregates, the mixture was slowly swirled to lift the sediment. To generate the converging flow field, the instrument was set up with a 0.8 mm inner diameter of glass capillary and silicon stopper connected to the sample cuvette. The glass capillary was placed in the O-ring filled with water on the slide glass which was then covered with a cover glass. A syringe pump (Fusion 200, Chemyx) was set at 5 mL/min of flow rate to create the converging flow for floc breakage. The broken flocs which flowed through the capillary were observed through the microscope. The flow valve was closed after the breakage of flocs to prevent re-aggregation between the broken aggregates. In the meantime, the images of the largest individual aggregates were taken for further analysis by using ImageJ 1.52a (Java 1.8.0 ver.). This software allows us to measure the maximum and minimum diameter (d_{maj} and d_{min}) of a floc as ellipsoidal.

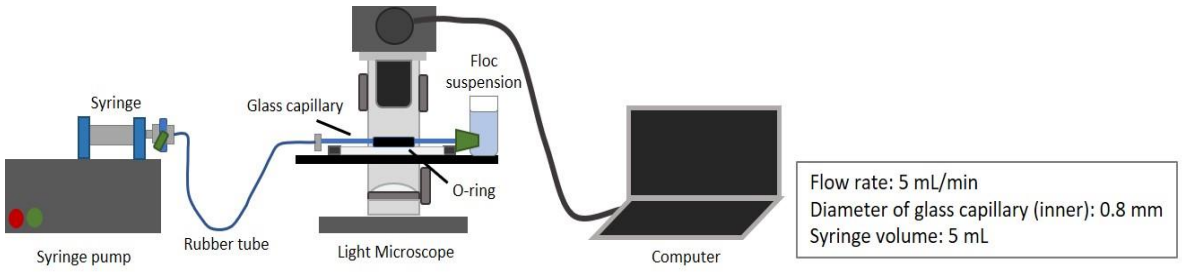

Figure 3.1. Schematic illustration of the breakage of protein-LHA aggregates by converging flow through a capillary of 0.8 mm in diameter. The flow rate used in this experiment is 5 mL/min (reuse from Khodir et al., 2020)

3.2.2.4 Calculation of floc strength

The assessment of floc strength against breakage followed the method by Kobayashi (Kobayashi 2005, 2004). Suppose the hydrodynamic force on the floc F_{hyd} is larger than the inner strength of the floc F_{floc}. In that case, there is a possibility of a floc breakage occurring

$$F_{hyd} \geq F_{floc} \tag{1}$$

When flocs are introduced to a converging flow to a capillary, floc breaks. The breakage resulted from a high elongation rate near the tube entrance during the converging flow. Kobayashi concluded that the overall floc size passed through the entrance is determined by the highest elongation rate along with the centerline $A_{c,max}$ to a capillary. The rate of elongation $A_{c,max}$ is provided by

$$A_{c,max} = \frac{3\sqrt{3}Q}{32\pi R^3} \tag{2}$$

where Q is the volumetric flow rate, and R is the capillary radius. The converging flow along the centerline is presumed as an axisymmetric straining flow. In an axisymmetric straining flow at an elongation rate A, Blaser (2000) demonstrated the hydrodynamic rupturing force with viscosity μ acting on an ellipsoidal floc with a surface area S as

$$F_{hyd} = \frac{C_{hyd} S \mu A}{2} \tag{3}$$

where the shape of the ellipsoids determines C_{hyd}. Consequently, the strength of the flocs is estimated from the maximum size of broken flocs. The major and minor lengths measure the floc surface area as an ellipsoid S (d_{maj} and d_{min}), portraying the maximum surface area as specified in the equation below of the best-fit ellipse S_{max} (Moriguchi, 1987)

$$S = 2\pi\left(\frac{ac^2}{\sqrt{c^2 - a^2}} \arccos\frac{a}{c}\right) \tag{4}$$

where $2a = d_{min}$ and $2c = d_{maj}$. Kobayashi (2005) listed C_{hyd} that can measure $(C_{hyd}S)_{max}$, which is the maximum $C_{hyd}S$ values of broken floc by the flow with $A_{c,max}$. Following all the consideration, the author concluded the equation for floc strength as below;

$$F_{floc} = \left(C_{hyd}S\right)_{max} \mu \frac{A_{c,max}}{2} \quad (5)$$

All the strength values in this investigation were evaluated using the equations described above.

3.3 Result and Discussion

3.3.1 Electrophoretic mobility of LSZ in the presence of Leonardite humic acid

3.3.1.1 Effect of ionic strength

The charging behavior of the LSZ-LHA complex can be investigated through electrophoretic mobility (EPM) as shown in Figure 3.2 as the function of KCl concentration and pH. The concentration ratio of LSZ to LHA used in this experiment was $C_{LSZ}/C_{LHA} = 2.5$. The LSZ-LHA complex is strongly influenced by pH. At low pH, it is caused by proton dissociation and deprotonation of amino acid side chain of LSZ and carboxylic groups of humic acid (Tan et al. 2008). At a higher pH region, the EPM resulted with negative mobility due to protonation and deprotonation processes controlled by functional groups (carboxyl group and amine) of LHA (Brigante et al. 2009). Hydrophobic interaction is also present in the complexation of protein and humic acid.

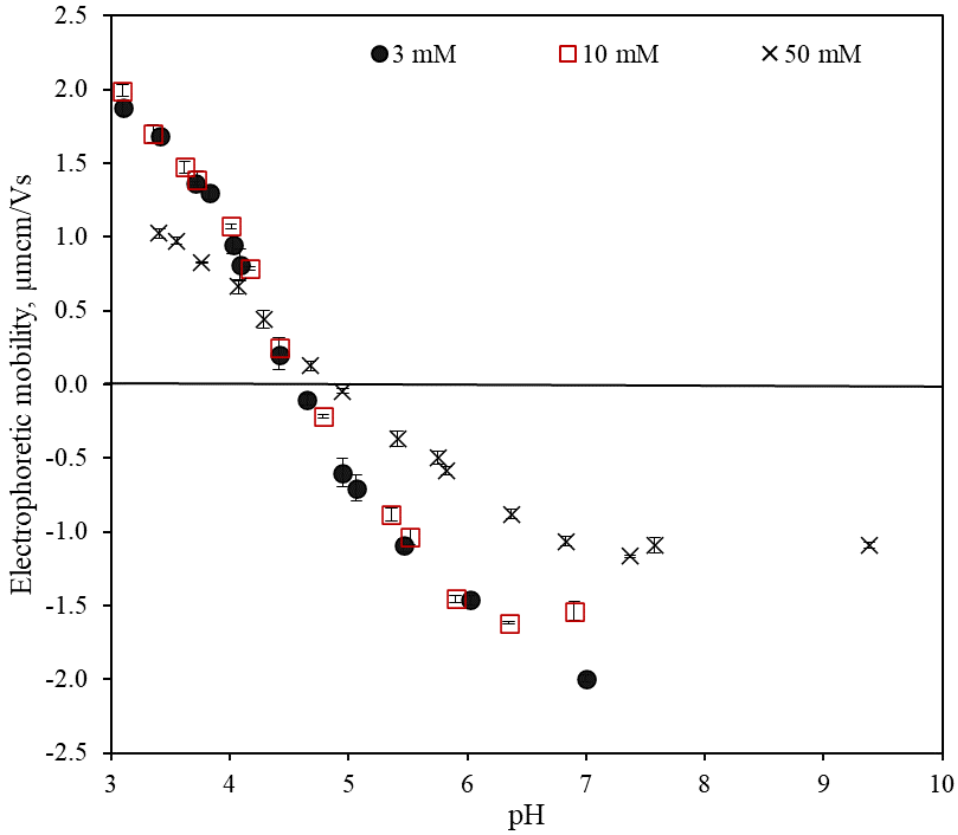

Figure 3.2. Electrophoretic mobility of the LSZ–LHA complex different KCl concentrations (3 mM, 10 mM, and 50 mM) as a function of pH. The suspension used are mass ratio 2.5. This data is reuse from Khodir et al. (2020)

3.3.1.2 Effect of mass ratio

We observe a charge inversion from positive to negative for mass ratio 2.5 and 5 at pH 4.5 and 7, resulting in Figure 3.3. This figure highlights the effect of surface charge on the interaction between these substances. The charge neutralization for mass ratio 2.5 has occurred at a much lower pH than mass ratio 5 due to the sufficient amount of LSZ to LHA concentration in the suspension. In mass ratio 5, while having a higher amount of LSZ than LHA, the IEP occurred at the later pH. The high amount of LSZ in the suspension as in mass ratio 5 can cause the repulsion between the protein substances. The repulsion leads to charge neutralization at the later pH, compared to mass ratio 2.5.

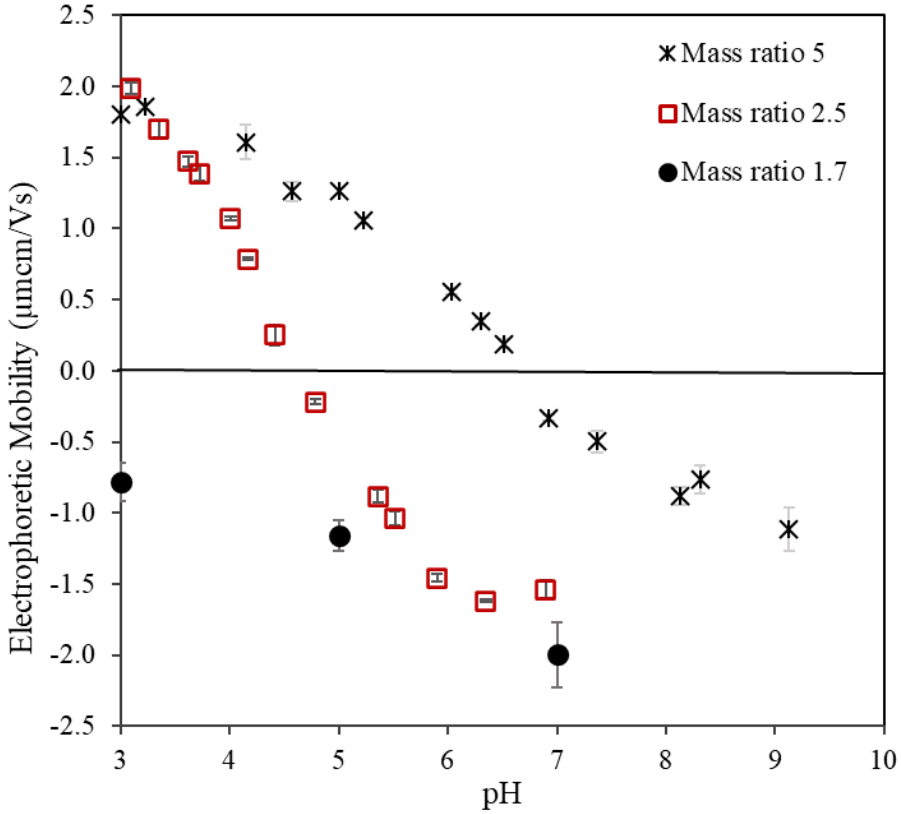

Figure 3.3. Electrophoretic mobility of the LSZ–LHA complex at 10 mM KCl complex as a function of pH. The EPM was measured at different mass ratios (1.7, 2.5, and 5). This figure is a reuse from Khodir et al. (2020)

3.3.2 Observation of LSZ-LHA aggregates

3.3.2.1 Effect of ionic strength

Figure 3.4 is the observation of the aggregation-dispersion process on the LSZ-LHA suspension. The aggregation was recorded to start in 2 hours, as shown in Figure 3.5. The appearance of aggregates outside the IEP region is not detectable by using EPM measurement only. This inspection shows that the aggregation and sedimentation took place at various pH (around pH 3 – 10) depending on the ionic strength. High KCl concentration has a much wider aggregation range than low KCl concentration. The appearance of floc for all KCl concentrations was confirmed from the microscopic observation.

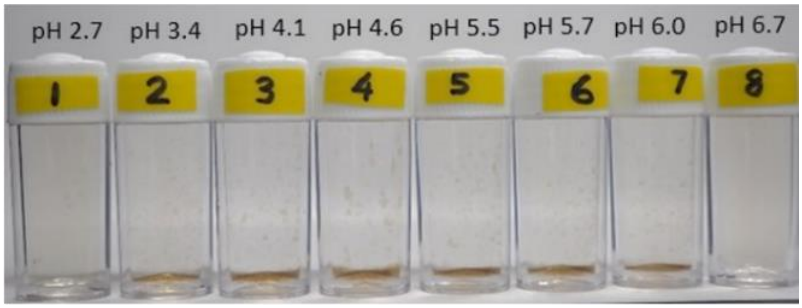

(A)

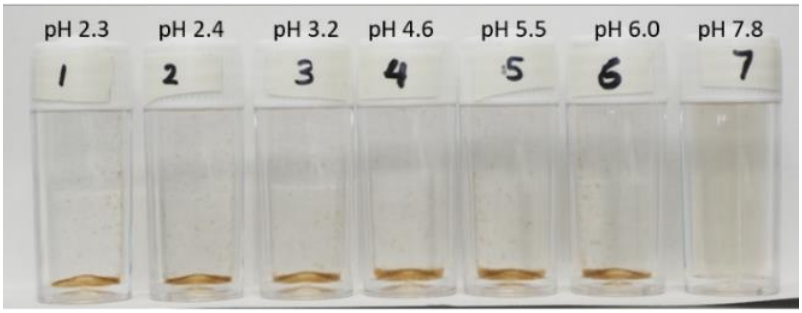

(B)

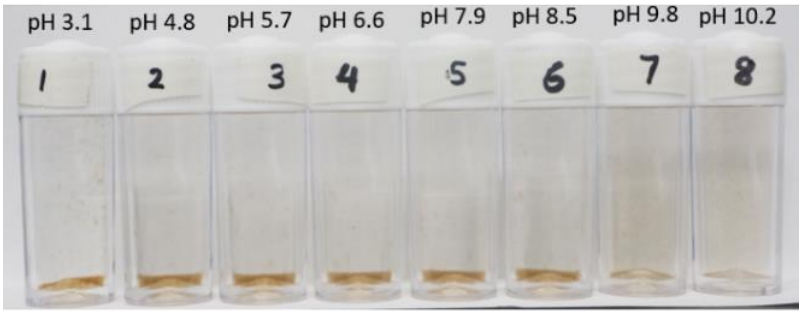

(C)

Figure 3.4. Aggregation and dispersion of LSZ and LHA complex on mass ratio C_{LSZ}/C_{LHA} = 2.5 as a function of pH at 3 mM (A), 10 mM (B), and 50 mM (C) of KCl concentration. The time frame for all images is at 24 hours. This figure is a reuse from Khodir et al. (2020)

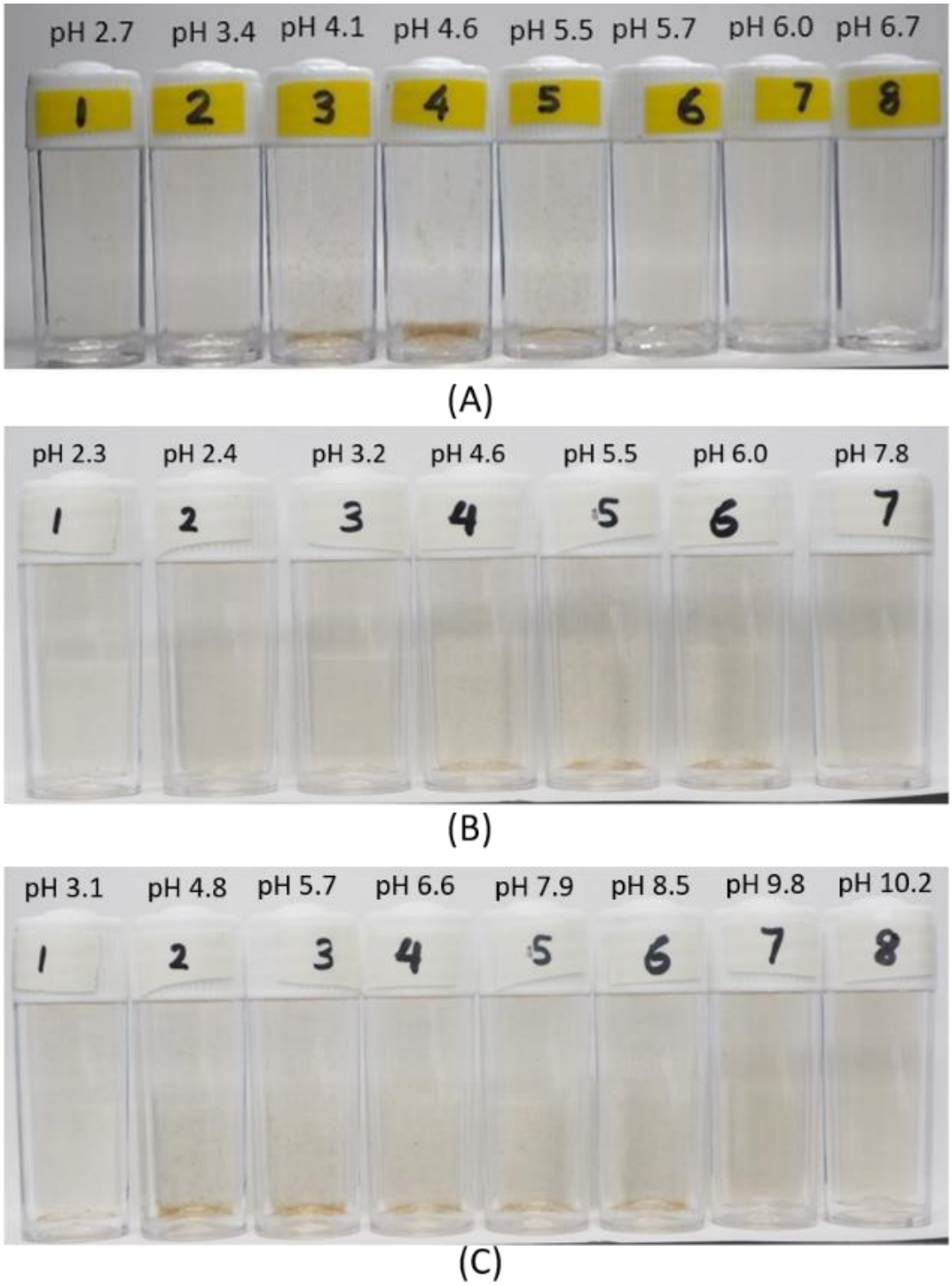

Figure 3.5. Early aggregation and dispersion process after 2 hours of observation. The LSZ-LHA complex used is mass ratio C_{LSZ}/C_{LHA} = 2.5 at 3 mM (A), 10 mM (B), and 50 mM (C) of KCl concentration. This figure is a reuse from Khodir et al. (2020).

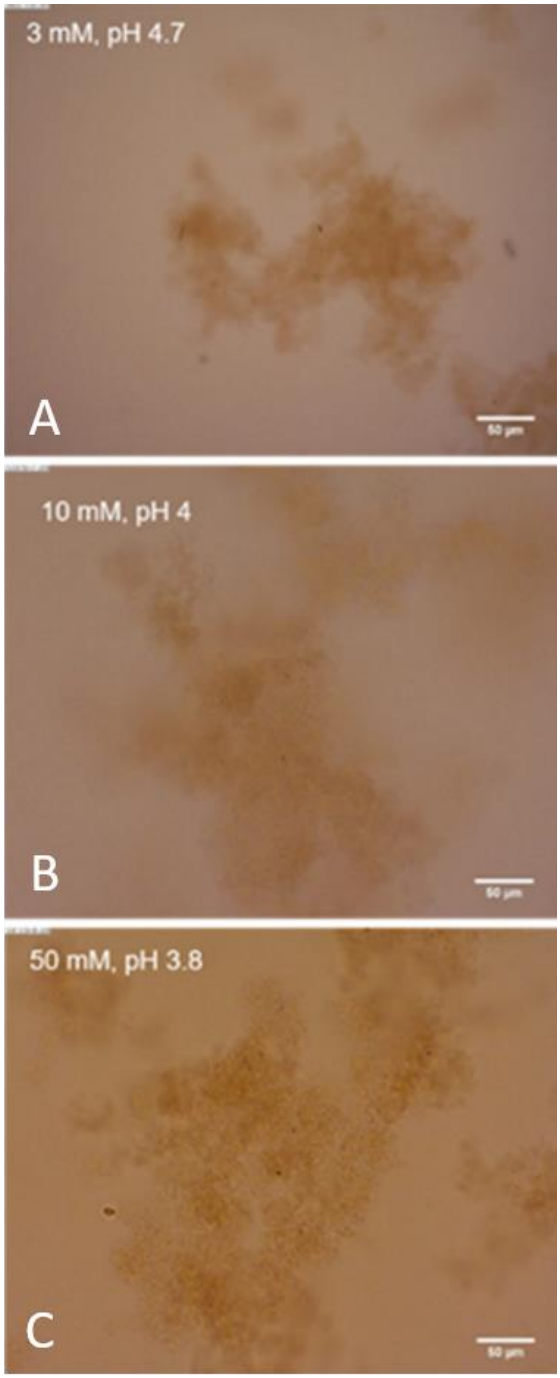

Figure 3.6. Microscopic view (20x magnification) on LSZ-LHA complex with mass ratio C_{LSZ}/C_{LHA} = 2.5 at 3 mM, 10 mM and 50 mM KCl concentration (A, B and C) (the scale bars indicate 50 μm). The pHs were at the charge neutralization region. This figure is a reuse from Khodir et al. (2020)

3.3.2.2 Effect of mass ratio

The observation of the LSZ-LHA suspension at different mass ratios was shown in Figures 3.6 and 3.7. The observation on mass ratio 5 was captured at different time frames. At hour 2, the aggregation appears near the isoelectric point (IEP). As the time passed (after 3

hours), the aggregation appears at the lower pH region. This observation was aligned with the floc strength data at the effect of mass ratio.

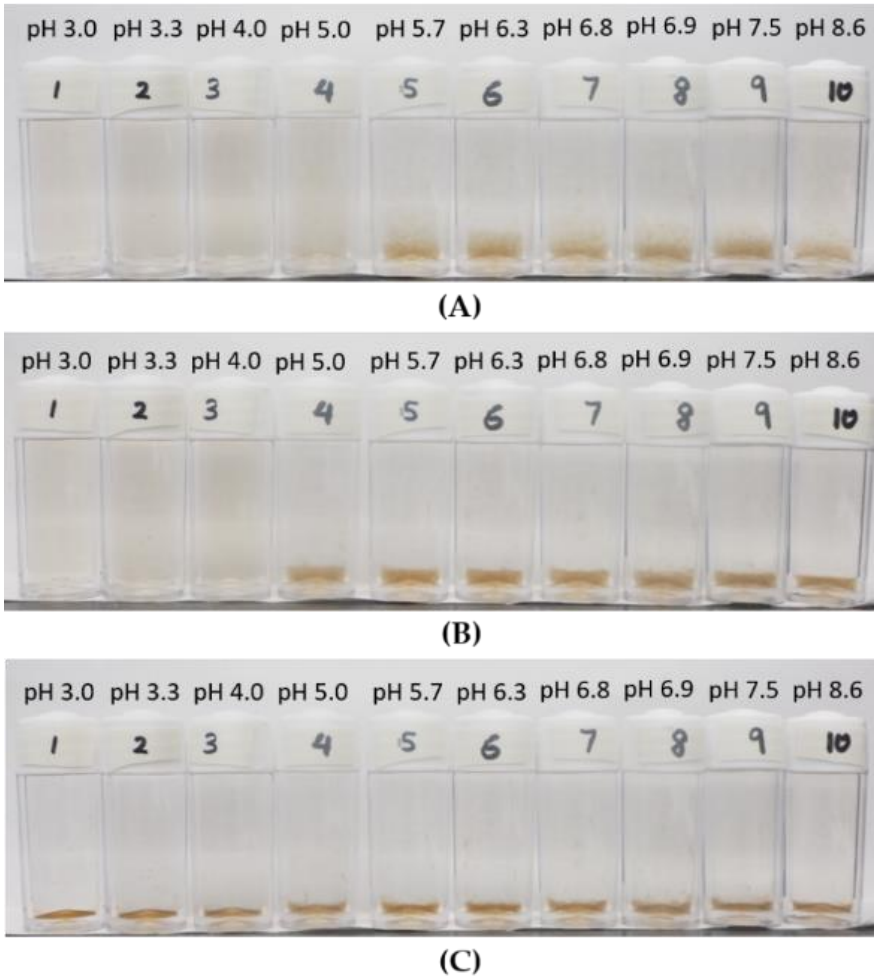

Figure 3.7. The observation of LSZ-LHA complex at mass ratio C_{LSZ}/C_{LHA} = 5 at 10 mM KCl concentration over pH. The time frame images are after 2 hours (A), after 3 hours (B) and after 24 hours (C). This figure is a reuse from Khodir et al. (2020)

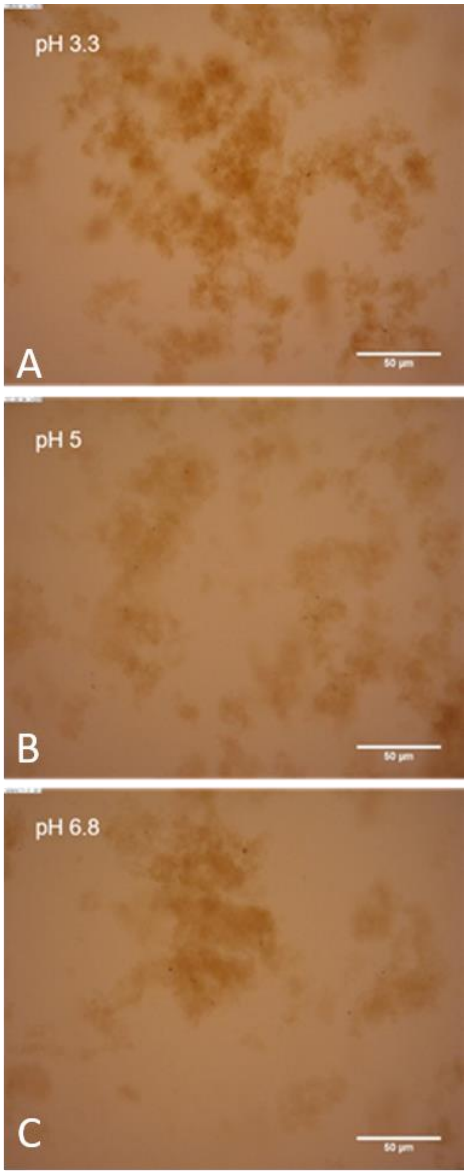

Figure 3.8. Microscopic view (20x magnification) on LSZ-LHA complex with mass ratio C_{LSZ}/C_{LHA} = 5 at 10 mM KCl concentration (the scale bars indicate 50 μm). This figure is a reuse from Khodir et al. (2020)

3.3.3 Floc strength of LSZ-LHA complex

3.3.3.1 Effect of ionic strength

We observed the low KCl concentration, 3 mM has the highest floc strength up to 4.5 nN, followed by 10 mM and 50 mM KCl with 3 nN and 2.8 nN. All of the floc strength was detected near the IEP range. The non-DLVO attraction called a charge patch was considered

to involve in the complexation of LS-LHA at the IEP region. At high salt concentration, this additional attraction diminished due to the double layer screening effect.

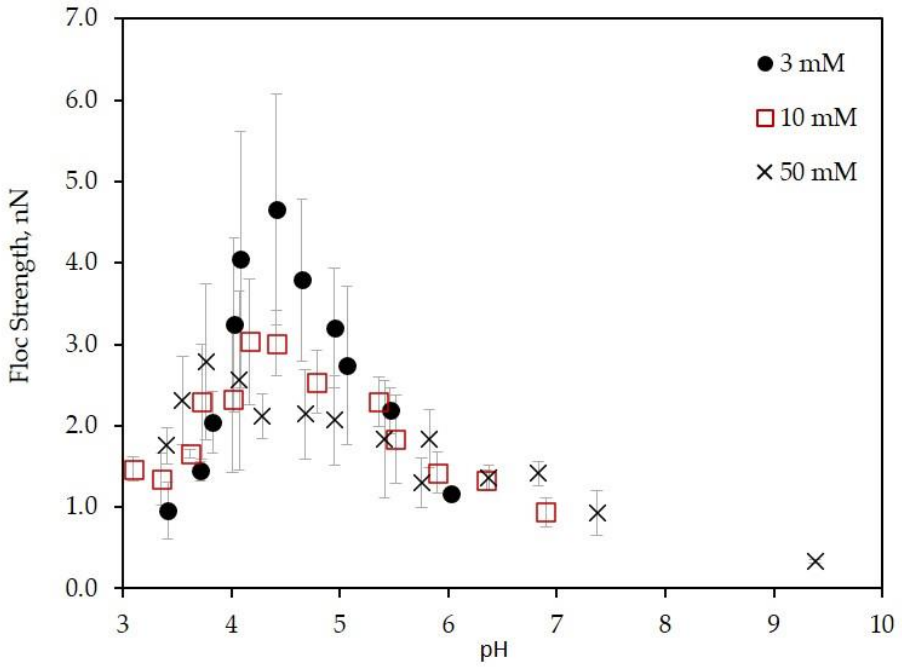

Figure 3.9. Floc strength of LSZ-LHA complex at different KCl concentrations (3 mM, 10 mM and 50 mM) as a function of pH. The LSZ-LHA complex measured at the mass ratio 2.5. This figure is a reuse from Khodir et al. (2020)

3.3.3.2 Effect of mass ratio

The present data shows the highest floc strength value up to 3 nN at the mass ratio of 2.5 and 5. Among all of the mass ratio (1.7, 2.5, and 5), mass ratio 5 displayed multiple peaks of floc strength over a pH range. The peaks appeared at both low and high pH regions with floc strength up to 2.3 nN and 3.2 nN for pH 4.2 and pH 7, correspondingly. The highest floc strength value (3.2 nN) at pH 7 is comparable to the peak of floc strength at a mass ratio 2.5. Besides, the floc strength value of mass ratio 1.7 is high up to 2.8 nN. This data makes the strength of flocs at the mass ratio 1.7 is comparable to the other mass ratios. With the previous floc strength data on the effect of KCl concentration and comparison to the EPM data (Figure

3.2), the highest strength value is initiated by the substantial attractive forces by charge neutralization.

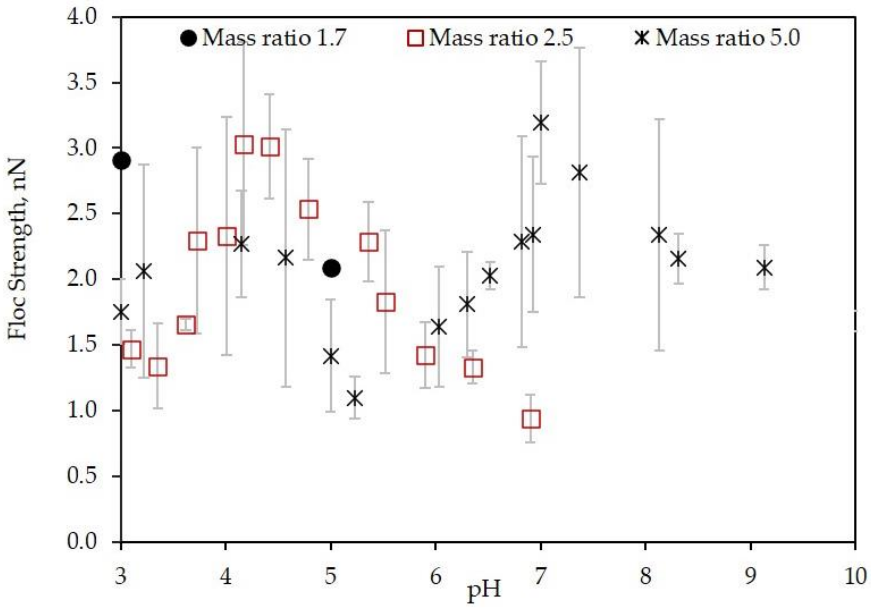

Figure 3.10. Floc strength of LSZ-LHA complex at different mass ratio (1.7, 2.5 and 5) as a function of pH. The KCl concentration used is 10 mM KCl. This figure is a reuse from Khodir et al. (2020)

3.4 Conclusion

This chapter aims to expand previous research and has produced a new way of analyzing the relationship between protein and humic acid. The quantitative assessment of the floc strength of lysozyme (LSZ) and leonardite humic acid (LHA) against breakage by converging flow is investigated as a function of ionic strength, pH, and mass ratio. The summary of this chapter is discussed below.

1) Confirmed the charge neutralization is the primary mechanism for the complexation of LSZ and LHA.

2) The highest floc strength was obtained at the lowest KCl concentration, 3 mM with 4.5 nN. The other KCl concentrations, 10 mM and 50 mM KCl detected to have 3 nN and 2.8 nN, respectively. The presence of charge-patch attraction helps strengthen the bonding between LSZ and LHA substances.

3) The effect of mass ratio, especially on mass ratio 5 has produced the highest floc strength up to 3.2 nN near the isoelectric point (IEP). This data is comparable with the floc strength of mass ratio 2.5. However, the mass ratio 5 produced a secondary peak at lower pH with 2.3 nN. The additional attraction could have strengthened the second peak bonding that overcame the strong repulsion force at the low pH region. Unfortunately, the reason remains unknown since a complex suspension is involved.

4 Aggregation of MO seed protein and humic acid particles: Floc strength

4.1 Introduction

NOM is a complex organic compound and one of the main contributors of bio-colloidal material in water. Depending on the climate, geology, and topography, the property and quantity of NOM in the water body vary (Matilainen et al. 2010) Besides, the presence of NOM is considered a significant problem to water quality. NOM has properties that can change the color, taste, and odor of water, especially in the water and wastewater treatment sector.

The aggregation-dispersion of NOM is commonly affected by several factors such as pH, salt concentrations, and particle concentration. The formation of flocs by the complex formation of NOM is discussed based on the Derjaguin-Landau-Verwey-Overbeek (DLVO) theory (Trefalt and Borkovec 2014). In water and wastewater treatments, the coagulant is used to enhance the aggregation process. The most common coagulant used is aluminum sulphate (alum) in the water treatment facility. Due to health concerns arising from alum usage, researchers focus more on the development of flocculants made of natural organic resources. Since decades ago, the *Moringa oleifera* (MO) seed has received much attention on its coagulation ability. Since the MO protein is extracted from the raw natural seed, the molecular weight of MO protein extract was reported to vary depending on the extraction and purification of protein (Baptista et al. 2017).

The aggregation-dispersion study on natural resource coagulants and their effectiveness in removing unwanted particles has been a major focus amongst the researchers. Flocs are prone to broken under high hydrodynamic force when the force is larger than the strength of the floc (Kobayashi et al. 1999; Jarvis et al. 2005). The evaluation of floc strength could help design water and wastewater treatment systems to achieve optimal turbidity removal. The complex conformation and fragility of the floc, however, make the evaluation of floc strength difficult. Therefore, we focus on the floc strength of the complex between MO seed protein

and humic acid. This chapter discussed the complexation and floc strength in terms of mass ratio, ionic strength, and pH.

4.2 Method

4.2.1 Electrophoretic mobility measurement

Electrophoretic mobility (EPM) measurement was measured by electrophoretic light scattering technique with Zetasizer Nano-ZS (Malvern). The measurements were carried out for MO-LHA complex at different KCl concentrations as a function of pH. The pH was adjusted with HCl and KOH solution. The concentration of MO protein used throughout the study were based on the grounded MO seed solution. KCl solution, HCl or KOH, deionized water, and lastly LHA solution were mixed into the 6 mL of a clear glass bottle. The bottle was inverted twice for let to stand 24 hrs. After 24 hrs, the suspension was injected into the measurement cell by using a syringe before the analysis. At the same time, pH was measured by using a pH meter (ELP-035, TOA DKK).

4.2.2 Observation of *Moringa oleifera* - humic acid aggregates

The preparation of MO-HA suspension was similar to the preparation of LSZ-LHA suspension. The aggregation and dispersion of MO-LHA suspension at different KCl concentrations and pH was observed macroscopically and microscopically. The macroscopic observation was taken by using a camera (Olympus PEN Lite, EPL 7) every 30 minutes in 24 hrs. Microscopic observation, on the other hand, was taken by using a light microscope (Shimadzu BA210E, Moticam 580INT) to capture the images of individual aggregates after 24 hrs of aggregation – sedimentation process.

4.2.3 Converging flow and floc breakage

The quantitative measurement of floc strength of MO – LHA aggregates at different KCl concentrations, 0.5 mM and 10 mM, were carried out from the floc breakage in a converging flow field. The construction and preparation of floc breakage through the converging flow field (Hakim et al. 2019; Hakim and Kobayashi 2019) was as displayed in Chapter 3.

4.2.4 Evaluation of floc strength

Floc strength assessment against breakage has been documented by Kobayashi (2005; 2004). If the hydrodynamic force on the floc is greater than the binding force of the floc, the breakup of a floc would potentially happen.

$$F_{\text{hyd}} \geq F_{\text{floc}} \tag{1}$$

Given the high elongation rate near the tube entrance, the added floc moves through a capillary by converging flow, and floc breakage occurs. Kobayashi considered that the highest elongation rate with the centerline $A_{\text{c, max}}$ to a capillary determined the maximum floc size. The rate of elongation $A_{\text{c, max}}$ is given by

$$A_{c,max} = \frac{3\sqrt{3}Q}{32\pi R^3} \tag{2}$$

where Q is the volumetric flow rate, and R is the capillary radius. The converging flow along the centerline is assumed as an axisymmetric straining flow. Blaser (2000) presented the hydrodynamic rupturing force in a fluid with viscosity μ. This hydrodynamic force act on an ellipsoidal floc with a surface area S in an axisymmetric straining flow at an elongation rate A as

$$F_{hyd} = \frac{C_{hyd} S \mu A}{2} \tag{3}$$

where C_{hyd} is determined by the shape of the ellipsoids. Consequently, the floc strength is defined from the largest size of broken flocs. The surface area of a floc as an ellipsoid S is determined by the major and minor lengths (d_{maj} and d_{min}) of floc. The measured floc resemble the maximum surface area of the best-fit Smax ellipsoids as defined in the equation below (Moriguchi, 1987)

$$S = 2\pi\left(\frac{ac^2}{\sqrt{c^2 - a^2}}\arccos\frac{a}{c}\right) \quad (4)$$

where $2a = d\text{min}$ and $2c = d\text{maj}$. Kobayashi (2005) has listed C_{hyd} which can be used to calculate $(C_{hyd}S)_{max}$. $(C_{hyd}S)_{max}$ is the maximum values of $C_{hyd}S$ of broken flocs by the flow with $A_{c,max}$. Following all the considerations, Kobayashi (2005) concluded the formula for floc strength as below;

$$F_{floc} = \left(C_{hyd}S\right)_{max}\mu\frac{A_{c,max}}{2} \quad (5)$$

All the strength values were evaluated using the above-described equations in this study.

4.3 Result and Discussion

4.3.1 Electrophoretic mobility of the MO-LHA complex

4.3.1.1 Effect of ionic strength

The electrophoretic mobility (EPM) of the MO-LHA complex at different KCl concentrations as a function of pH is shown in Figure 4.2. The complexes have a strong influence on pH but have a weak influence on ionic strength. Between 0.5 mM and 10 mM KCl, there are no differences in mobility magnitude.

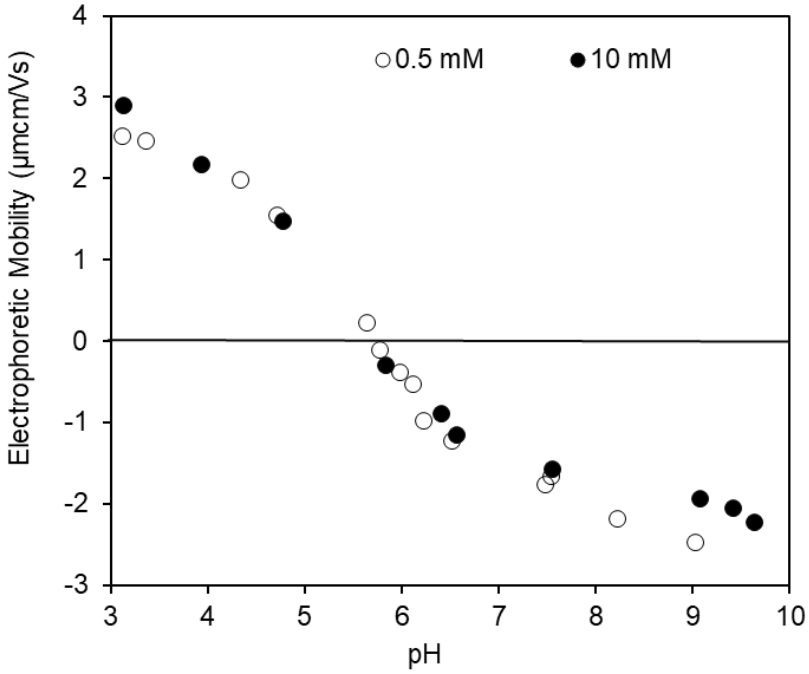

Figure 4.1. Electrophoretic mobility of the MO-LHA complex with mass ratio 5 at different KCl concentrations (0.5 mM and 10 mM) against pH

4.3.1.2 Effect of mass ratio

The EPM of the MO-LHA complex at different mass ratios is shown as a function of pH in Figure 4.3. The mass ratio 5 has 0.5 mM and 10 mM KCl concentration; meanwhile, mass ratio 2.5 displayed for 10 mM KCl only. Note the EPM of mass ratio 5 in Figure 4.3 is similar to Figure 4.2. The EPM at mass ratio 2.5 and 5 have similar mobility of charge inversion from positive to negative mobility along with the pH ranges. However, the EPM at mass ratio 5 has greater mobility compared to mass ratio 2.5. The IEP for mass ratio 5 is at pH 5.6 while, mass ratio 2.5 has IEP at pH 4, respectively. The difference in magnitude mobility demonstrates the effect of MO protein concentration and charges.

`

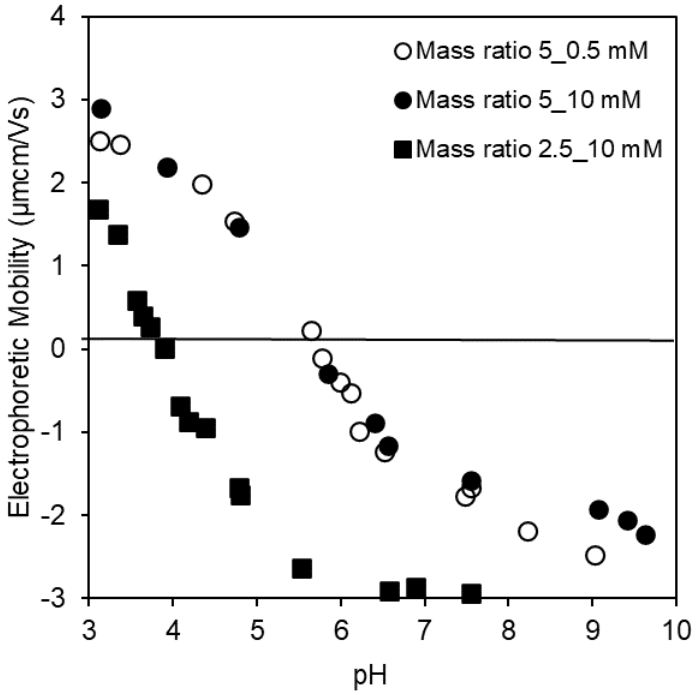

Figure 4.2. Electrophoretic mobility of the MO-LHA complex as the function of pH in 10 mM KCl at different mass ratios (2.5 and 5)

4.3.2 Macroscopic and microscopic observation on MO-LHA complex

Macroscopic and microscopic observations were carried out to verify the aggregation-dispersion of MO-LHA suspension at the mass ratio 2.5 and 5 with 10 mM KCl concentration, as shown in Figures 4.4 and 4.5. The observation was executed at different pHs. The clear sediment started to appear near the IEP region, pH 3.9 and pH 5.8 for mass ratio 2.5 and 5. The aggregation region between mass ratio 2.5 and 5 are different and observed at a different time frame. Mass ratio 2.5 aggregated towards lower pH, meanwhile, mass ratio 5 aggregated towards higher pH. This observation for both mass ratios can be compared with the EPM data n Figure 4.3. The microscopic observation in Figure 4.6 shows the presence of floc at the IEP region.

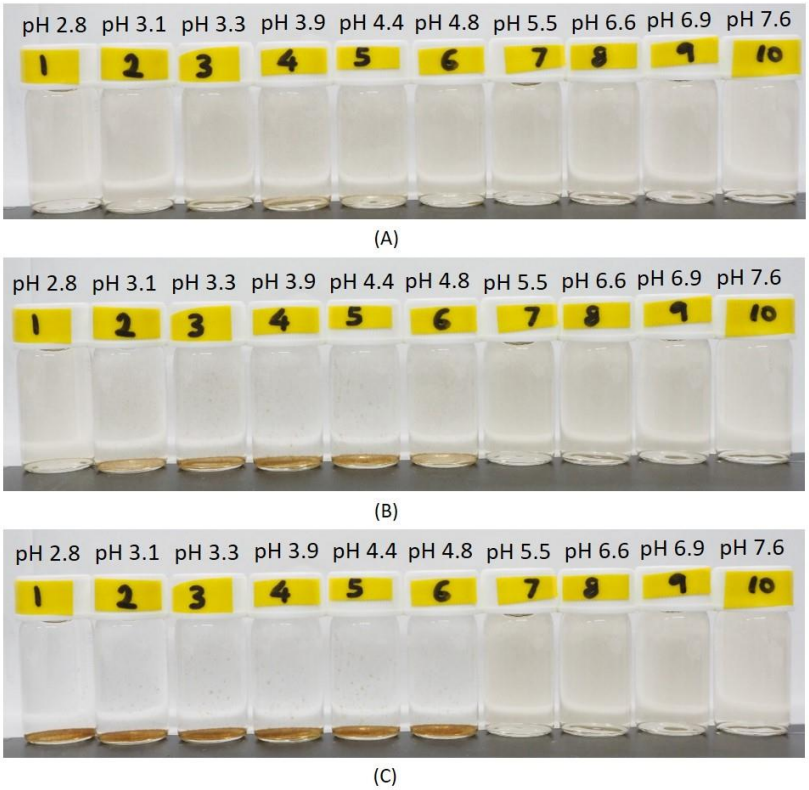

Figure 4.3. Macroscopic observation of MO-LHA complex at mass ratio C_{MO}/C_{LHA} = 2.5 at 10 mM KCl concentration over pH. The time frame for each image were 2.5 hrs (A), 5 hrs (B), and 24 hrs (C).

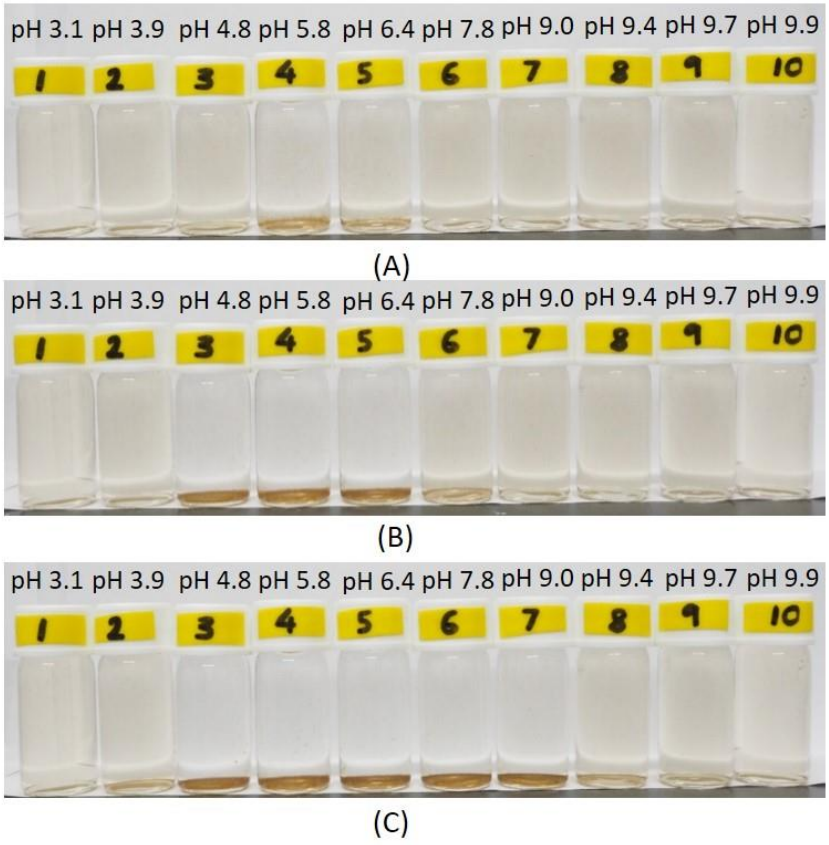

Figure 4.4. Macroscopic observation of MO-LHA complex at mass ratio C_{MO}/C_{LHA} = 5 at 10 mM KCl concentration over pH. The time frame of each images taken was 2 hrs (A), 5.5 hrs (B), and 24 hrs (C).

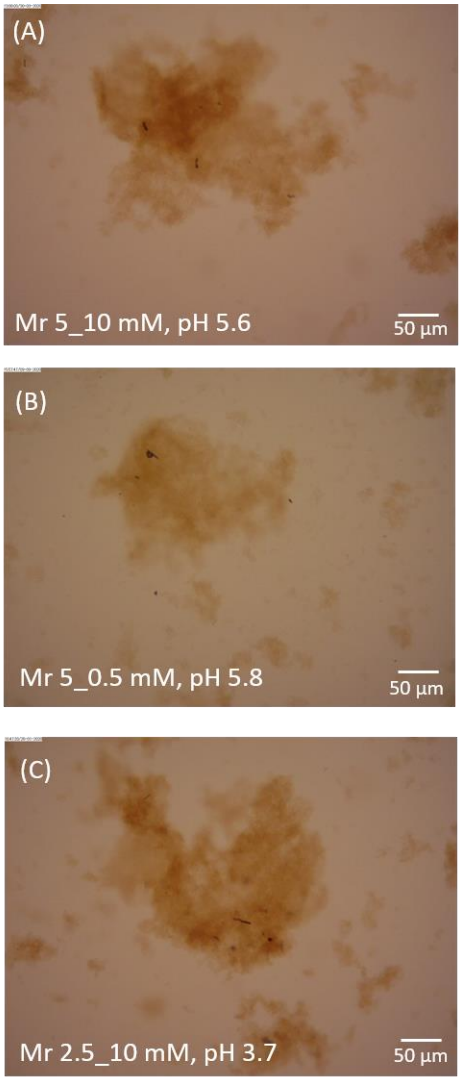

Figure 4.5. Microscopic images of individual aggregates at mass ratio C_{MO}/C_{LHA} = 5 with different KCl concentration; 10 mM KCl (A) and 0.5 mM KCl (B), and mass ratio C_{MO}/C_{LHA} = 2.5 at 10 mM KCl (C). The images were taken at the isoelectric point (IEP). Mr indicates for mass ratio in this figure.

4.3.3 Floc strength of MO-LHA complex

The highest floc strength was observed for low KCl concentration, 0.5 mM up to 6.4 nN. Additional charge-patch attraction was detected to be involved in strengthening the floc bonding near the IEP region. At high KCl concentration, this additional attraction was not detected due to the double-layer screening effect. Comparing the floc strength of the MO-LHA complex and LSZ-LHA complex, the MO-LHA complex has much stronger bonding. The adsorption of MO seed protein somehow leads to a stronger binding with LHA substances.

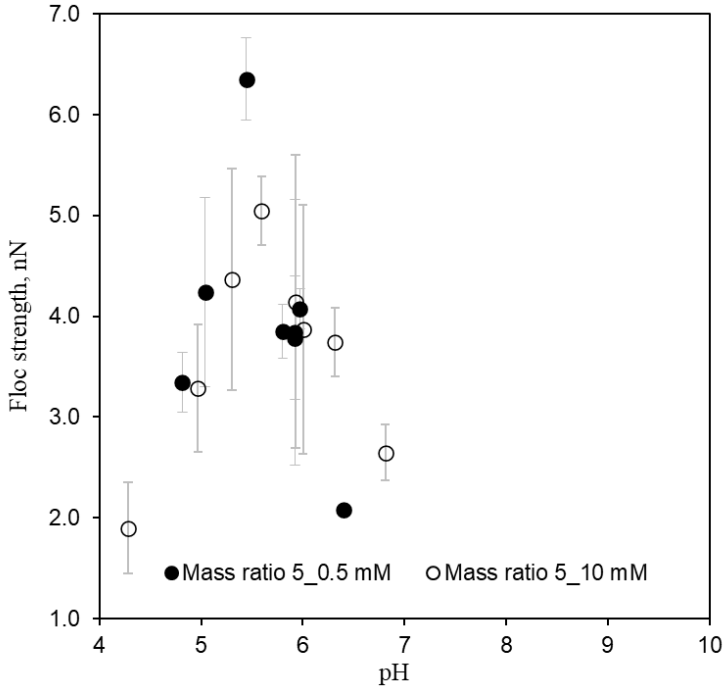

Figure 4.6. Floc strength of MO-LHA complex with mass ratio C_{MO}/C_{LHA} = 5 as a function of KCl concentrations (0.5 mM and 10 mM) as a function of pH

4.4 Conclusion

Chapter 4 discussed the evaluation data on the floc strength between *Moringa oleifera* (MO) seed protein and Leonardite humic acid (LHA) floc. The floc strength of the complexes was measured under the converging flow field and evaluated for the effect of mass ratio, pH, and ionic strength. The summary of this chapter is discussed below.

1) The charge neutralization was confirmed as the primary mechanism in the complexation of MO seed protein and LHA. The EPM data has shown charge reversal from positive to negative charge with the increased pH.

2) The floc strength of the MO-LHA complex was obtained up to 6.4 nN for 0.5 mM KCl, and 5.05 nN for 10 mM KCl, respectively. Additional charge-patch attraction helps strengthen the floc bond.

3)The MO-LHA complexes have resulted in stronger binding of floc compared to the LSZ-LHA complex.

5 Conclusion

In chapter 1 explains the general information regarding the colloidal particles and their transportation through the soil pore. There are many colloidal and nanosized particles and macromolecules in soil and water environments, such as clays, humic substances, and proteins. Colloidal matters can aggregate and form flocs depending on water chemistry and the interaction among different substances. Ionic strength, pH, and concentration of colloidal are some of the parameters that influenced the interaction. This interaction could affect the transport properties of a floc. A large and dense floc settle down in water and deposit within soil pore. Meanwhile, a small aggregate will travel around the environment. The strength of flocs depends on the inter-substance binding forces in the aggregates to hold the flocs together (Parker 1972; Bache et al. 1997). The floc strength is also referring to the number of individual bonds and their strength within the flocs. The aggregates and flocs are subjected to breakage in flow fields when the hydrodynamic force is larger than the strength of aggregates/flocs. A strength studies on a floc have become attention by the previous researchers. One of the astounding pieces of research is the measurement of floc strength through a converging flow system. The first study was conducted by Kobayashi (2005) on the polystyrene microsphere. The author was able to obtain 2nN of floc strength. The floc strength research has recently studied several colloidal complexes such as humic substance (hakim) and humic substances with protein (Khodir et al. 2020). Proteins and humic substances are essential components in soil and water environments. The aggregation-dispersion study on complex organic material such as protein and humic substances is challenging and limited compared to inorganic substances. Understanding the transportation of complex substances through the soil pore with the water flow is crucial. Besides, the fate of substances in environments can be predicted and control. Studies on the complexation of proteins and humic substances were reported by (Tan et al. 2008). However, the strength of these complex substances has never been reported.

Therefore, we have determined to study the aggregation and flocs' strength formed by the complexation of proteins and humic substances. This study compares commercialized protein and plant-based protein in terms of complexation with humic acid and floc strength.

In chapter 2, we characterized each substance used in the research. The information is either obtained through experiments or extracted from the literature. Our research used standard humic substances, Leonardite humic acid (LHA), from International Humic Substances Society (IHSS). LHA has been used due to its higher possibility of aggregation from its hydrophobicity and has produced stronger floc than Suwannee River fulvic acid (Hakim and Kobayashi 2019; Hakim et al. 2019). We have selected two types of protein to be used in our research, Lysozyme (LSZ) and *Moringa oleifera* (MO) protein. LSZ protein is a model protein because of its stability. MO seed protein, which has attracted attention as a natural eco-friendly flocculant, has also been investigated. The properties of used natural proteins and humic acid are also summarized. The surface charge of proteins and humic acid (LHA) under the effect of ionic strength and pH are crucially important when considering their complexation. We obtained that the charging of all substances is easily influenced by pH and ionic strength. Under a pH range, the functional groups of LSZ, MO seed protein, and LHA are subjected to deprotonation and protonation. The zeta potential calculated using the Smoluchowski equation has found the relaxation effect on MO protein solution at a function of pH. Since the MO seed protein was extracted during the experiment, the size of the substance needs to be analyzed. The hydrodynamic size of MO seed protein increased with the pH. At low pH, the size of MO seed protein is 24.17 nm and 6.66 nm for condition (i) no second filtration and condition (ii) with the second filtration. The observation of the MO seed protein has confirmed the formation of aggregates at high pH.

Chapter 3 summarized the complexation of LSZ and humic acid was studied in terms of their charging behavior, aggregation-dispersion, and floc strength. The complexation,

aggregation, and dispersion of colloidal particles could be affected by hydrophobic, van der Waals, and electrostatic interactions. The experiments were performed in different ionic strength and LSZ-LHA mass ratios as a function of pH. We obtained the stronger flocs at pH 4.4, where the isoelectric point (IEP) of the complex with the mass ratio of 2.5 was confirmed. Thus, the aggregation of LSZ–LHA flocs is mainly caused by charge neutralization. We obtained the floc strength of 4.7 nN around IEP at a low salt concentration of 3 mM, which was more potent than 2.8 nN in a high salt concentration of 50 mM. The effect of salt concentration can be rationalized by charge-patch attraction at low salt concentration. With increasing mass ratio, the IEP shifted to higher pH. This is due to the increase in positive charge from LSZ in the mixture. The effect of the LSZ to LHA mass ratio on the maximum strength was weak in the range studied. The aggregation-dispersion of LSZ-LHA suspension was observed macroscopically and microscopically. We detected the formation of aggregates that were beyond the IEP range. The interaction between the range of charge neutralization would be hydrophobic, hydrogen bonding, and adsorption.

Chapter 4 shows the result with MO protein, which is a natural coagulant recently receiving attention on its properties. To check the aggregation capability of MO protein, we decided to check the charging behavior and aggregation-dispersion of the MO-LHA complex. I have studied flocs' formation and strength by the complexation of MO and humic acid (LHA). The experiment was performed at different ionic strength and MO protein to LHA mass ratios as a function of pH. In this experiment, we obtained MO-LHA flocs' strength at low salt concentration with 6.4 nN, stronger than the LSZ-LHA flocs. The strongest floc was found to occur at the IEP range. The binding forces strengthened between flocs at low salt concentration cannot be explained by Derjaguin, Landau, Verwey, and Overbeek (DLVO) theory. An additional non-DLVO force called a charge patch is accountable for this mechanism. The highest MO obtained this highest floc strength to LHA mass ratio. The effect of particle

concentration on the MO-LHA complex was more obvious. The observation on the aggregation-dispersion behavior was found to show aggregation beyond the IEP range as well.

Chapter 5 summarizes the findings in this thesis. The evaluation on the protein – humic acid flocs were performed by charging behavior, observation of individual aggregates, and floc strength under the effect of ionic strength and the mass ratio at the function of pH. The formation of aggregates is mainly by charge neutralization, where additional attractive forces are found. This force has strengthened the binding between the flocs even though the ionic strength was low. Other forces occurred outside the IEP range and help with the aggregation. However, some problem is unavoidable, such as the properties of MO seed protein that depended on the extraction method. The evaluation of floc strength also needs an improvement to reduce the time and error during the handling.

5.1 Future research perspective

Here includes the future perspective of this research.

5.1.1 Floc strength measurement

The evaluation of floc strength was performed with a designated instrument. A proper handling method is needed to improve the evaluation of floc strength. The error bar was high while doing this experiment due to the handling and the suspension. The aggregation-dispersion for each suspension might not be the same, and since the observation was performed microscopically, a little different uncontrolled operation could affect the size of aggregates.

5.1.2 Identification and characterization of *Moringa oleifera* seed protein

A more extensive research is required for characterization of MO seed protein since there are a wide range of proteins exists from the seed. Simplified and standardized methods on the protein extraction are required to avoid confusion on the properties of protein.

APPENDICES A

Chapter 2: Characterization of Proteins and Humic acid

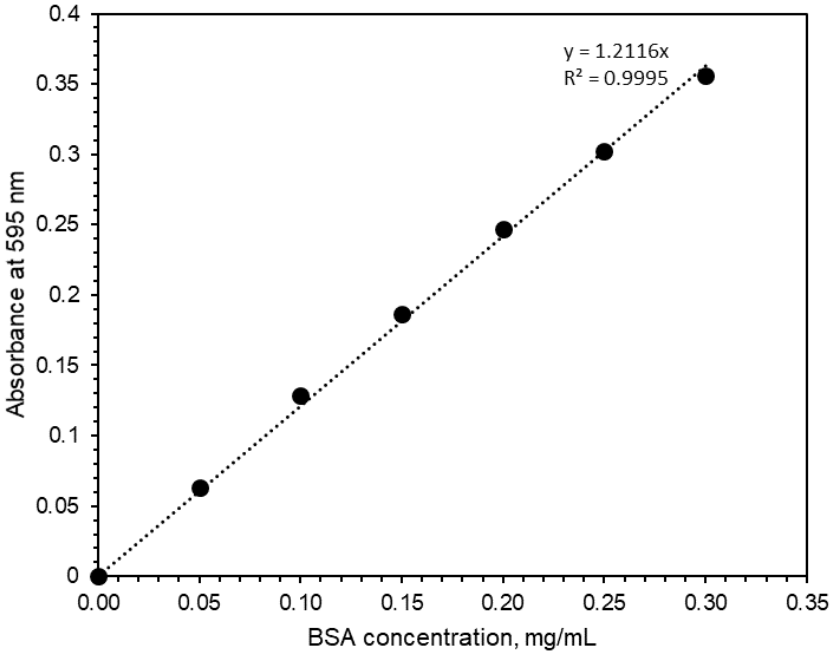

Figure A1. Standard curve of different concentration of BSA protein standard. The curve was measured at absorbance 595 nm by the Bradford assay method. The MO seed suspension used was without the second filtration.

Table A1. Dynamic light scattering (DLS) of bare MO protein and with the addition of KCl concentrations (0.5 mM, 1.0 mM, 10 mM, and 50 mM). The concentration of MO solution is 2.4 g/L (w/v).

KCl concentration (mM)	Z-average diameter (nm)	Polydisperse Index (PDI)	pH
MO only	5.84	0.26	4.6
0.5	7.76	0.33	4.6
1	33.30	0.13	4.6
10	42.09	0.34	4.6
50	133.61	0.39	4.6

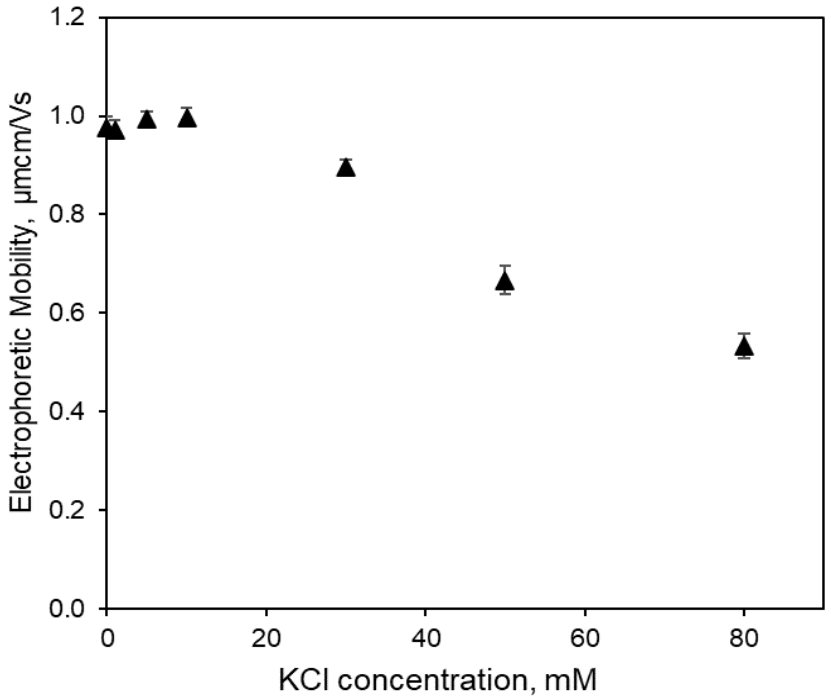

Figure A2. Electrophoretic mobility of 2.4 g/L (w/v) of MO seed suspension as a function of KCl concentration. The suspension was measured with pH 4.6 for all KCl concentration.

Figure A3 showed the weak dependency of ionic strength below 20 mM KCl. The addition of KCl in the MO suspension can cause the screening of repulsion forces on the surface of MO substances. This screening effect causes the MO substances to aggregate and increases in size.

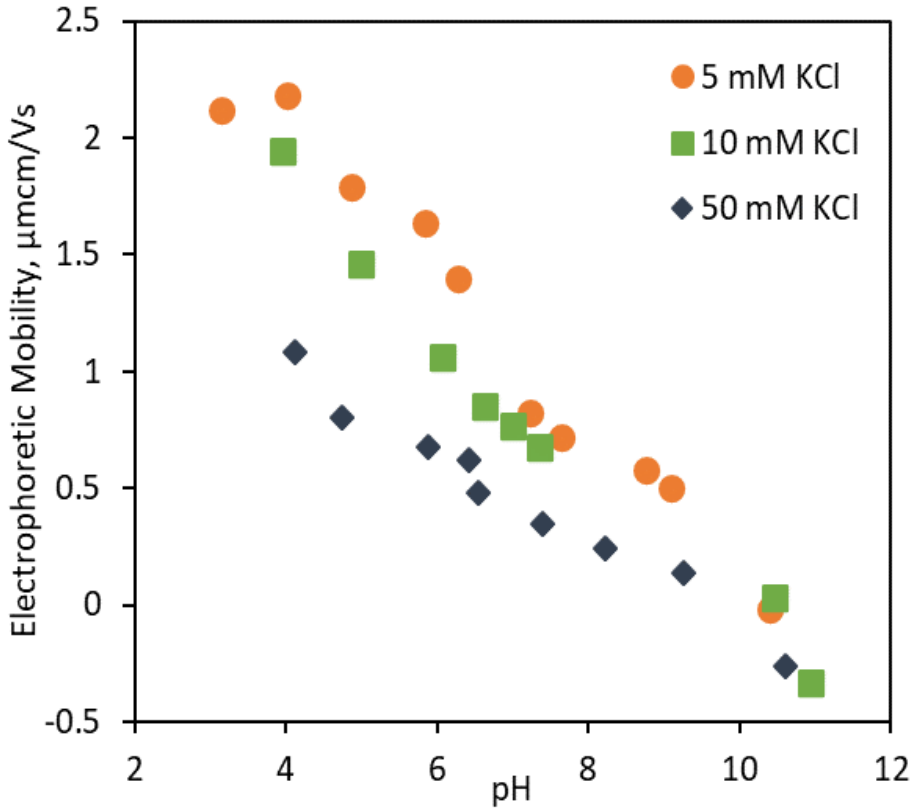

Figure A3. Electrophoretic mobility of LSZ suspension at different KCl concentration (5 mM, 10 mM, and 50 mM) as a function of pH. This data is extracted from Yamaguchi and Kobayashi (2016).

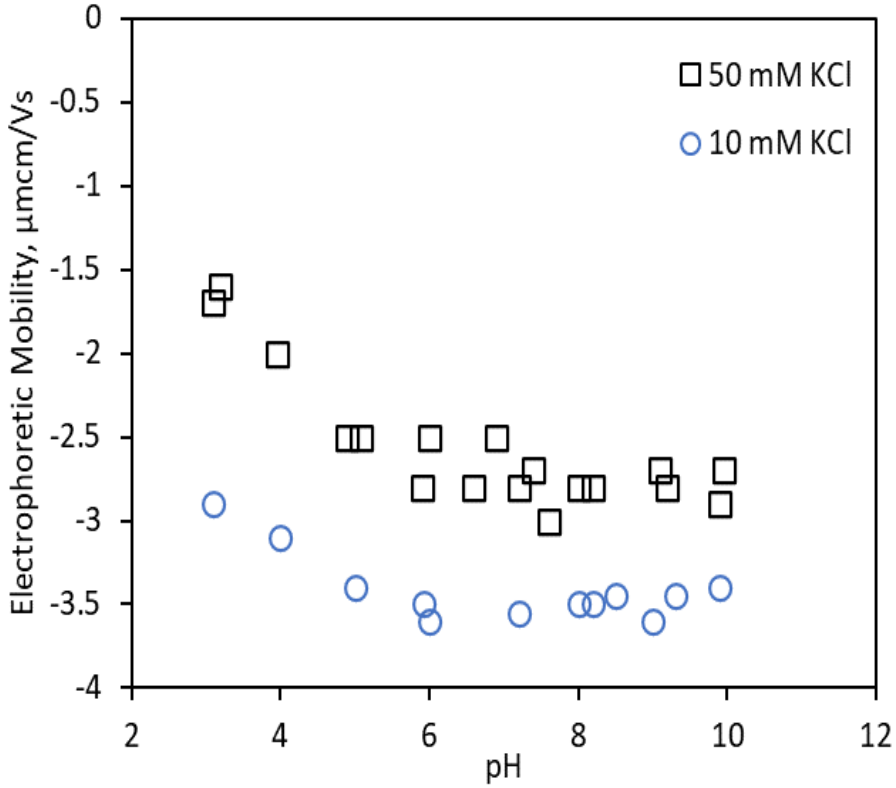

Figure A4. Electrophoretic mobility of Leonardite humic acid (LHA) at different KCl concentration (10 mM, and 50 mM) as a function of pH. This data is extracted from Hakim and Kobayashi (2018).

Appendix B

Table B1. Debye length of different KCl concentrations (3 mM, 10 mM and 50 mM) use in the LSZ-LHA system.

KCl concentration (mM)	1.	3	2.	10	3.	50
Debye Length (nm)	4.	5.55	5.	3.04	6.	1.36

References

Abd Wahid, Muhamad Azhar, Megat Johari Megat Mohd Noor, Masafumi Goto, Norio Sugiura, Nor'azizi Othman, Zuriati Zakaria, Thamer Ahmad Mohammed, Ahmad Jusoh, and Hirofumi Hara. 2017. "Recombinant Protein Expression of Moringa Oleifera Lectin in Methylotrophic Yeast as Active Coagulant for Sustainable High Turbid Water Treatment." *Bioscience, Biotechnology and Biochemistry* 81 (8): 1642–49. https://doi.org/10.1080/09168451.2017.1329617.

Agrawal, Himesh, Chandan Shee, and Ashwani K. Sharma. 2007. "Isolation of a 66 KDa Protein with Coagulation Activity from Seeds of Moringa Oleifera." *Research Journal of Agriculture and Biological Sciences* 3 (5): 418–21.

Avena, Marcelo J., and Kevin J. Wilkinson. 2002. "Disaggregation Kinetics of a Peat Humic Acid: Mechanism and PH Effects." *Environmental Science and Technology* 36 (23): 5100–5105. https://doi.org/10.1021/es025582u.

Bache, D. H., C. Johnson, J. F. McGilligan, and E. Rasool. 1997. "A Conceptual View of Floc Structure in the Sweep Floc Domain." *Water Science and Technology* 36 (4): 49–56. https://doi.org/10.1016/S0273-1223(97)00418-6.

Baptista, Aline Takaoka Alves, Mariana Oliveira Silva, Raquel Guttierres Gomes, Rosângela Bergamasco, Marcelo Fernandes Vieira, and Angélica Marquetotti Salcedo Vieira. 2017. "Protein Fractionation of Seeds of

Moringa Oleifera Lam and Its Application in Superficial Water Treatment." *Separation and Purification Technology* 180: 114–24. https://doi.org/10.1016/j.seppur.2017.02.040.

Beltrán-Heredia, J, and J Sánchez-Martín. 2009. "Removal of Sodium Lauryl Sulphate by Coagulation/Flocculation with Moringa Oleifera Seed Extract." *Journal of Hazardous Materials* 164 (2–3): 713–19. https://doi.org/10.1016/j.jhazmat.2008.08.053.

Blaser, Stefan. 2000. "Break-up of Flocs in Contraction and Swirling Flows." *Colloids and Surfaces A: Physicochemical and Engineering Aspects* 166 (1–3): 215–23. https://doi.org/10.1016/S0927-7757(99)00450-1.

Brigante, Maximiliano, Graciela Zanini, and Marcelo Avena. 2009. "Effect of PH, Anions and Cations on the Dissolution Kinetics of Humic Acid Particles." *Colloids and Surfaces A: Physicochemical and Engineering Aspects* 347 (1–3): 180–86. https://doi.org/10.1016/j.colsurfa.2009.04.003.

Bünemann, Else K., Giulia Bongiorno, Zhanguo Bai, Rachel E. Creamer, Gerlinde De Deyn, Ron de Goede, Luuk Fleskens, et al. 2018. "Soil Quality – A Critical Review." *Soil Biology and Biochemistry* 120 (February): 105–25. https://doi.org/10.1016/j.soilbio.2018.01.030.

Denny S. Parker, Proj. Engr.; Brown and Caldwell. 1972. "Floc Breakup in Turbulent Flocculation Processes." *Ournal of the Sanitary Engineering*

Division Vol. 98 (Issue 1): Pg. 79-99. https://cedb.asce.org/CEDBsearch/record.jsp?dockey=0127407.

Gassenschmidt, U, K D Jany, B Tauscher, and H Niebergall. 1995. “Isolation and Characterization of a Flocculating Protein from Moringa Oleifera Lam.” *Biochimica et Biophysica Acta* 1243 (3): 477–81. https://doi.org/10.1016/0304-4165(94)00176-X.

Ghebremichael, Kebreab A., K. R. Gunaratna, Hongbin Henriksson, Harry Brumer, and Gunnel Dalhammar. 2005. “A Simple Purification and Activity Assay of the Coagulant Protein from Moringa Oleifera Seed.” *Water Research* 39 (11): 2338–44. https://doi.org/10.1016/j.watres.2005.04.012.

Giachin, Gabriele, Joanna Narkiewicz, Denis Scaini, Ai Tran Ngoc, Alja Margon, Paolo Sequi, Liviana Leita, and Giuseppe Legname. 2014. “Prion Protein Interaction with Soil Humic Substances: Environmental Implications.” *PLoS ONE* 9 (6). https://doi.org/10.1371/journal.pone.0100016.

Giachin, Gabriele, Ridvan Nepravishta, Walter Mandaliti, Sonia Melino, Alja Margon, Denis Scaini, Pierluigi Mazzei, et al. 2017. “The Mechanisms of Humic Substances Self-Assembly with Biological Molecules: The Case Study of the Prion Protein.” *PLoS ONE* 12 (11): 1–16. https://doi.org/10.1371/journal.pone.0188308.

Hakim, Azizul, and Motoyoshi Kobayashi. 2018. “Aggregation and Charge

Reversal of Humic Substances in the Presence of Hydrophobic Monovalent Counter-Ions: Effect of Hydrophobicity of Humic Substances." *Colloids and Surfaces A: Physicochemical and Engineering Aspects* 540 (November 2017): 1–10. https://doi.org/10.1016/j.colsurfa.2017.12.065.

———. 2019. "Charging, Aggregation, and Aggregate Strength of Humic Substances in the Presence of Cationic Surfactants: Effects of Humic Substances Hydrophobicity and Surfactant Tail Length." *Colloids and Surfaces A: Physicochemical and Engineering Aspects* 577 (May): 175–84. https://doi.org/10.1016/j.colsurfa.2019.05.071.

Hakim, Azizul, Tomoharu Suzuki, and Motoyoshi Kobayashi. 2019. "Strength of Humic Acid Aggregates: Effects of Divalent Cations and Solution PH." Research-article. *ACS Omega* 4 (5): 8559–67. https://doi.org/10.1021/acsomega.9b00124.

Hogg, Richard. 2012. "Bridging Flocculation by Polymers." *KONA Powder and Particle Journal* 30 (30): 3–14. https://doi.org/10.14356/kona.2013005.

Jarvis, P., B. Jefferson, J. Gregory, and S. A. Parsons. 2005. "A Review of Floc Strength and Breakage." *Water Research*. https://doi.org/10.1016/j.watres.2005.05.022.

Katchalsky, Aharon, and Pnina Spitnik. 1947. "Potentiometric Titrations of Polymethacrylic Acid." *Journal of Polymer Science* 2 (5): 487–487.

https://doi.org/10.1002/pol.1947.120020504.

Katre, Uma V., C. G. Suresh, M. Islam Khan, and Sushama M. Gaikwad. 2008. "Structure-Activity Relationship of a Hemagglutinin from Moringa Oleifera Seeds." *International Journal of Biological Macromolecules* 42 (2): 203–7. https://doi.org/10.1016/j.ijbiomac.2007.10.024.

Khodir, Wan Khairunnisa Wan Abdul, Azizul Hakim, and Motoyoshi Kobayashi. 2020. "Strength of Flocs Formed by the Complexation of Lysozyme with Leonardite Humic Acid." *Polymers* 12 (8): 14–16. https://doi.org/10.3390/polym12081770.

Kobayashi, Motoyoshi. 2004. "Breakup and Strength of Polystyrene Latex Flocs Subjected to a Converging Flow." *Colloids and Surfaces A: Physicochemical and Engineering Aspects* 235 (1–3): 73–78. https://doi.org/10.1016/j.colsurfa.2004.01.008.

———. 2005. "Strength of Natural Soil Flocs." *Water Research* 39 (14): 3273–78. https://doi.org/10.1016/j.watres.2005.05.037.

———. 2008. "Electrophoretic Mobility of Latex Spheres in the Presence of Divalent Ions: Experiments and Modeling." *Colloid and Polymer Science* 286 (8–9): 935–40. https://doi.org/10.1007/s00396-008-1851-9.

Kobayashi, Motoyoshi, Yasuhisa Adachi, and Setsuo Ooi. 1999. "Breakup of Fractal Flocs in a Turbulent Flow." *Langmuir* 15 (13): 4351–56.

https://doi.org/10.1021/la980763o.

Kuehner, Daniel E., Jan Engmann, Florian Fergg, Meredith Wernick, Harvey W. Blanch, and John M. Prausnitz. 1999. “Lysozyme Net Charge and Ion Binding in Concentrated Aqueous Electrolyte Solutions.” *The Journal of Physical Chemistry B* 103 (8): 1368–74. https://doi.org/10.1021/jp983852i.

Li, Yan, Luuk K. Koopal, Juan Xiong, Mingxia Wang, Chenfeng Yang, and Wenfeng Tan. 2018. “Influence of Humic Acid on Transport, Deposition and Activity of Lysozyme in Quartz Sand.” *Environmental Pollution* 242: 298–306. https://doi.org/10.1016/j.envpol.2018.06.096.

Li, Yan, Wenfeng Tan, Luuk K. Koopal, Mingxia Wang, Fan Liu, and Willem Norde. 2013. “Influence of Soil Humic and Fulvic Acid on the Activity and Stability of Lysozyme and Urease.” *Environmental Science and Technology* 47 (10): 5050–56. https://doi.org/10.1021/es3053027.

Ma, Jie, Huaming Guo, Liping Weng, Yongtao Li, Mei Lei, and Yali Chen. 2018. “Chemosphere Distinct Effect of Humic Acid on Ferrihydrite Colloid-Facilitated Transport of Arsenic in Saturated Media at Different PH.” *Chemosphere* 212: 794–801. https://doi.org/10.1016/j.chemosphere.2018.08.131.

Matilainen, Anu, Mikko Veps??l??inen, and Mika Sillanp???? 2010. “Natural Organic Matter Removal by Coagulation during Drinking Water Treatment:

A Review.” *Advances in Colloid and Interface Science* 159 (2): 189–97. https://doi.org/10.1016/j.cis.2010.06.007.

Ndabigengesere, Anselme, K. Subba Narasiah, and Brian G. Talbot. 1995. “Active Agents and Mechanism of Coagulation of Turbid Waters Using Moringa Oleifera.” *Water Research* 29 (2): 703–10. https://doi.org/10.1016/0043-1354(94)00161-Y.

Nurul, mas’ud waqiah. 2013. “済無No Title No Title.” *Persepsi Masyarakat Terhadap Perawatan Ortodontik Yang Dilakukan Oleh Pihak Non Profesional* 53 (9): 1689–99.

Okuda, T., A. U. Baes, W. Nishijima, and M. Okada. 2001. “Isolation and Characterization of Coagulant Extracted from Moringa Oleifera Seed by Salt Solution.” *Water Research* 35 (2): 405–10. https://doi.org/10.1016/S0043-1354(00)00290-6.

Ouyang, Y., D. Shinde, R. S. Mansell, and W. Harris. 1996. “Colloid-Enhanced Transport of Chemicals in Subsurface Environments: A Review.” *Critical Reviews in Environmental Science and Technology* 26 (2): 189–204. https://doi.org/10.1080/10643389609388490.

Pota, Giulio, Virginia Venezia, Giuseppe Vitiello, Paola Di Donato, Valentina Mollo, Aniello Costantini, Joshua Avossa, et al. 2020. “Tuning Functional Behavior of Humic Acids through Interactions with Stöber Silica

Nanoparticles.” *Polymers* 12 (4). https://doi.org/10.3390/polym12040982.

Rigou, Peggy, Human Rezaei, Jeanne Grosclaude, Siobhán Staunton, and Hervé Quiquampoix. 2006. “Fate of Prions in Soil: Adsorption and Extraction by Electroelution of Recombinant Ovine Prion Protein from Montmorillonite and Natural Soils.” *Environmental Science and Technology* 40 (5): 1497–1503. https://doi.org/10.1021/es0516965.

Ritchie, Jason D., and E. Michael Perdue. 2003. “Proton-Binding Study of Standard and Reference Fulvic Acids, Humic Acids, and Natural Organic Matter.” *Geochimica et Cosmochimica Acta* 67 (1): 85–96. https://doi.org/10.1016/S0016-7037(02)01044-X.

S. Moriguchi. n.d. “Mathematical Formulas (Sugaku Koshikishu).”

Santos, a F S, a C C Argolo, L C B B Coelho, and P M G Paiva. 2005. “Detection of Water Soluble Lectin and Antioxidant Component from Moringa Oleifera Seeds.” *Water Research* 39 (6): 975–80. https://doi.org/10.1016/j.watres.2004.12.016.

Santos, A F S, M G Carneiro-da-Cunha, J A Teixeira, P M G Paiva, L C B B Coelho, and R Nogueira. 2011. “Interaction of Moringa Oleifera Seed Lectin with Humic Acid.” *Chemical Papers* 65 (4): 406–11. https://doi.org/DOI 10.2478/s11696-011-0025-2.

Santos, Andréa F.S., Luciana a. Luz, Adriana C.C. Argolo, José a. Teixeira,

Patrıícia M.G. Paiva, and Luana C.B.B. Coelho. 2009. “Isolation of a Seed Coagulant Moringa Oleifera Lectin.” *Process Biochemistry* 44 (4): 504–8. https://doi.org/10.1016/j.procbio.2009.01.002.

Tan, W. F., L. K. Koopal, L. P. Weng, W. H. van Riemsdijk, and W. Norde. 2008. “Humic Acid Protein Complexation.” *Geochimica et Cosmochimica Acta* 72 (8): 2090–99. https://doi.org/10.1016/j.gca.2008.02.009.

Trefalt, Gregor, and Michal Borkovec. 2014. “Overview of DLVO Theory.” *Laboratory of Colloid and Surface Chemistry, University of Geneva*, 1–10. www.colloid.ch/dlvo.

Ueda Yamaguchi, Natália, Luís Fernando Cusioli, Heloise Beatriz Quesada, Maria Eliana Camargo Ferreira, Márcia Regina Fagundes-Klen, Angélica Marquetotti Salcedo Vieira, Raquel Guttierres Gomes, Marcelo Fernandes Vieira, and Rosângela Bergamasco. 2020. “A Review of Moringa Oleifera Seeds in Water Treatment: Trends and Future Challenges.” *Process Safety and Environmental Protection* 147: 405–20. https://doi.org/10.1016/j.psep.2020.09.044.

Xu, Weiying, Baoyu Gao, Qinyan Yue, and Xiaowen Bo. 2011. “Influence of PH on Flocs Formation , Breakage and Fractal Properties — The Role of Al 13 Polymer.” *Journal of Water Sustainability* 1 (1): 45–57. https://doi.org/10.11912/jws.1.1.45-57.

Yamaguchi, Atsushi, and Motoyoshi Kobayashi. 2016. “Quantitative Evaluation of Shift of Slipping Plane and Counterion Binding to Lysozyme by Electrophoresis Method.” *Colloid and Polymer Science* 294 (6): 1019–26. https://doi.org/10.1007/s00396-016-3852-4.